Trans-Cis Photoisomerization of the Stilbenes and a Reexamination of the Positional Dependence of the Heavy-Atom Effect[1]

Jack Saltiel,* Al Marinari, David W.-L. Chang, James C. Mitchener, and E. Dennis Megarity[2]

Contribution from the Department of Chemistry, The Florida State University, Tallahassee, Florida 32306. *Received August 25, 1978*

Abstract: Larger azulene quenching effects are observed on trans → cis quantum yields than on trans/cis photostationary compositions for the direct photoisomerization of the stilbenes and the *p*-, *m*-, and *m,m'*-bromine substituted derivatives. Analysis of these data together with the temperature dependence of fluorescence quantum yields for each trans isomer in *n*-pentane indicates that (1) intersystem crossing yields based on photostationary states can be unreliable, (2) the singlet mechanism ($^1t^* \rightarrow {}^1p^*$) is confirmed as the major isomerization pathway of *trans*-stilbene singlets, (3) significant fractions of bromostilbene $^1t^*$ molecules intersystem cross, (4) almost all bromostilbene singlets ($\phi_{is}{}^1p^* \geq 0.60$) intersystem cross following twisting to $^1p^*$, and (5) the positional dependence previously inferred for the heavy-atom effect is incorrect. Azulene effects on the cis → trans and the cis → DHP photoisomerizations are reported. The photoisomerization mechanism for the *cis*-bromostilbenes cannot involve $^1p^*$ as an exclusive intermediate. A pathway involving excited dihydrophenanthrenes is tentatively proposed.

There have been several investigations concerning the effect of heavy-atom substitution on the behavior of electronically excited stilbene molecules.[3-7] Comparison of the temperature dependence of fluorescence, ϕ_f, and isomerization, $\phi_{t\rightarrow c}$ and $\phi_{c\rightarrow t}$, quantum yields for the stilbenes and the *p*-halostilbenes revealed a substantial bromine substituent effect.[3-5] Increasing the temperature in the parent hydrocarbon from −180 to 25 °C increases $\phi_{t\rightarrow c}$ while decreasing ϕ_f, these two processes being coupled throughout the temperature range.[4,5,7-9] In *p*-bromostilbene $\phi_{t\rightarrow c}$ is reported to be temperature independent while ϕ_f increases modestly as the temperature is decreased.[3,4] Bromine substitution brings into play an additional pathway for stilbene photoisomerization which is generally assigned to heavy atom enhanced intersystem crossing.[3-5,7] The temperature dependence of $\phi_{c\rightarrow t}$ in the systems studied is not informative concerning possible differences in behavior between excited *cis*-stilbene and its halogen-substituted derivatives. However, halogen substitution, especially in the meta position, has been reported to lower $\phi_{c\rightarrow t}$ significantly and it has been suggested that enhanced spin-orbit coupling induces very rapid $^1c^* \rightarrow {}^3c^* \rightarrow {}^1c$ decay.[6,10] This suggestion contradicts the commonly expressed view that, with the exception of a small cyclization component to dihydrophenanthrene (DHP) in the singlet state, torsion about the central bond to twisted geometries, $^1p^*$ and $^3p^*$, is the major decay mode of cis excited states.[7]

In assigning minor, if any, importance to the triplet path for the direct photoisomerization of the unsubstituted stilbenes, the ability of azulene to intercept stilbene triplets has been relied upon heavily.[11] The aim of this research was to extend the use of azulene as a mechanistic probe under direct excitation conditions to the bromostilbenes, where triplet intermediates were strongly suspected.[12] Schulte-Frohlinde and co-workers have extended the method to several *p*-nitrostilbenes.[13,14] Initial inferences concerning the effect of bromine substitutions were based on azulene effects on cis-trans photostationary compositions which suggested that, as in stilbene itself, little or no intersystem crossing occurs in the *m*-bromo- and the *m,m'*-dibromostilbenes, but that intersystem crossing is a significant decay channel in the *p*-bromostilbenes.[12] The marked differences in the temperature dependence of ϕ_f and $\phi_{t\rightarrow c}$ of *trans*-stilbene and *trans*-*p*-bromostilbene are consistent with these conclusions,[3,4,7] but no fluorescence data bearing on the apparent striking positional dependence of bromine's influence on $S_1 \rightarrow T_1$ spin-orbit coupling were available. In this paper such data are reported along with azulene effects on photostationary states and photoisomerization quantum yields. These results require some modification of the conclusions which were based solely on photostationary measurements.

Results

Photochemical Observations. Photostationary states for the benzophenone-sensitized isomerization of the stilbenes with and without added azulene in *n*-pentane and in benzene are shown in Table I. Photostationary states for the direct isomerization of the bromostilbenes in *n*-pentane and in benzene in the presence of azulene using 313-nm excitation are shown in Table II. Results for the *m,m'*-dibromostilbenes from similar experiments in *n*-pentane but with added alkenes or mossy zinc are shown in Table III. Photostationary states for the direct excitation of the stilbenes in *n*-pentane in the presence of azulene using 254-nm excitation are shown in Table IV.

Relative photoisomerization conversions for the benzophenone-sensitized isomerization of the *p*-bromostilbenes in benzene are shown in Table V. These are converted to *quantum yields* using the benzophenone-sensitized photoisomerization of *cis*-stilbene, $\phi_{c\rightarrow t} = 0.41$,[15,16] for actinometry. No complications due to bromine atom formation were encountered in the benzophenone-sensitized isomerizations.

Several sets of experiments were carried out in which relative photoisomerization conversions were measured in the presence of mossy zinc using 313-nm excitation and the benzophenone-sensitized photoisomerization of *cis*-1,3-pentadiene (*c*-P) for actinometry, $\phi_{c\rightarrow t} = 0.55$.[17,18] Typical results are shown in Table VI. Prolonged irradiations, 313 nm, in the presence of mossy zinc, but without visible excitation to minimize concentrations of dihydrophenanthrenes, led to side products whose GLC retention times are consistent with assignment to the corresponding phenanthrenes. Conversions to these products for a set of samples which was irradiated in parallel follow: St (10 ± 5%), *p*-BrSt (45%), *m*-BrSt (6.5 ± 2%), and *m,m'*-diBrSt (50 ± 2%). Small GLC peaks corresponding to replacement of bromine by hydrogen were also observed. Direct excitation photostationary states, obtained in the absence of mossy zinc or azulene for the bromostilbenes, were generally very rich in the trans isomers. Since azulene appears to be an efficient scavenger of bromine atoms it was used for that purpose in preliminary quantum yield measurements with 254-nm excitation in *n*-pentane. Assuming $\phi_{t\rightarrow c} = 0.49$ for *trans*-stilbene a $\phi_{c\rightarrow t} = 0.36$ was obtained and in parallel irradiations for the *p*-bromostilbenes $\phi_{t\rightarrow c} = 0.21$ and 0.28 and

0002-7863/79/1501-2982$01.00/0

Table I. Azulene Effect on Photostationary States of Benzophenone-Sensitized Stilbene Isomerization, 30 °C[a]

n-pentane		benzene	
[Az], M × 10^2	% $[t]_s$	[Az], M × 10^2	% $[t]_s$
	Stilbene		
0	37.0 ± 0.2	0	41.2 ± 0.5
0.76	63.7 ± 0.3	1.13	61.4 ± 0.6
1.52	76.0 ± 0.2	2.24	71.4 ± 0.2
2.49	82.9 ± 0.2	3.21	77.6 ± 0.6
	p-Bromostilbene		
0	40.6 ± 0.2	0	43.4 ± 0.4
0.50	45.2 ± 0.2	0.25	44.2 ± 0.2
0.90	49.4 ± 0.4	0.50	47.3 ± 0.3
1.25	52.7 ± 0.2	0.75	48.9 ± 0.2
2.00	48.2 ± 0.3	1.25	52.0 ± 0.2
2.50	61.5 ± 0.4	2.00	55.9 ± 0.2
		2.50	47.7 ± 0.2
	m-Bromostilbene		
0	43.3 ± 1.2[b]	0.76	64.4 ± 0.3
0.25_1	52.9 ± 1.1	1.52	72.6 ± 0.3
0.49_5	59.4 ± 0.5	2.28	76.9 ± 1.0
0.77_2	61.5 ± 0.7	3.03	79.9 ± 0.9
1.54	72.4 ± 0.4		
2.32	76.8 ± 0.2		
3.05	81.3 ± 0.4		
	m,m'-Dibromostilbene		
0	37.9 ± 1.0[c]	0	42.6 ± 0.2
0.75	70.2 ± 0.4	1.54	77.1 ± 0.4
1.51	81.9 ± 0.5	3.09	85.1 ± 0.2
2.26	86.9 ± 1.0	4.63	88.4 ± 0.4
3.02	88.8 ± 0.3	6.18	90.3 ± 0.3

[a] Benzophenone 0.05 M throughout. Substrate concentrations in the order presented follow: *n*-pentane, 0.0198, 0.0100, 0.0103, 0.0100 M; benzene, 0.0183, 0.0100, 0.0108, 0.0100 M. Filter system 1 was employed. [b] Prolonged irradiation gave rise to product having GLC retention time somewhat longer than that of trans isomer. [c] Several other products (~20%) were present (GLC analyses).

Table II. Azulene Effect on Photostationary States of Direct Stilbene Isomerization, 30 °C, 313 nm[a]

n-pentane		benzene	
[Az], M × 10^2	% $[t]_s$	[Az], M × 10^2	% $[t]_s$
	p-Bromostilbene		
0.50	12.4 ± 0.2	0.50	16.4 ± 0.2
0.90	13.7 ± 0.2	0.90	17.1 ± 0.2
1.25	14.4 ± 0.4	1.25	18.1 ± 0.2
2.00	16.4 ± 0.3	1.70	19.2 ± 0.2
2.50	18.0 ± 0.2	2.00	19.9 ± 0.1
		2.50	20.8 ± 0.3
	m-Bromostilbene[b]		
0.76	12.3 ± 0.3	0.76	13.6 ± 0.2
1.52	13.0 ± 0.2	1.52	14.6 ± 0.2
2.28	14.0 ± 0.2	2.28	15.7 ± 0.2
3.03	14.9 ± 0.2	3.03	16.4 ± 0.1
	m,m'-Dibromostilbene[b]		
0.77	8.0 ± 0.2	1.54	15.1 ± 0.2
1.54	10.3 ± 0.1	3.09	16.3 ± 0.3
2.31	12.3 ± 0.3	4.63	21.0 ± 0.2
3.08	13.9 ± 0.4	6.18	22.2 ± 0.2

[a] Stilbene concentrations in the order presented follow: *n*-pentane, 0.0100, 0.0103, 0.0063 M; benzene, 0.0100, 0.0109, 0.099 M. Filter system 2 employed unless otherwise indicated. [b] For *m*-bromostilbene in *n*-pentane and *m,m'*-dibromostilbene in benzene identical observations were obtained using filter systems 2 and 3.

$\phi_{c\rightarrow t}$ = 0.53 and 0.45 for 10^{-4} and 10^{-3} M azulene, respectively.

The effect of azulene on 313-nm direct trans → cis isomerization conversions for the stilbenes is shown in Table VII. 1-Hexene and/or mossy zinc were included in bromostilbene ampules. Identical irradiation conditions and time periods were employed for experiments in which 1-hexene was also included. For these experiments conversions obtained in the absence of azulene are related approximately to the $\phi_{t\rightarrow c}$ quantum yields in Table VI. Assuming $\phi_{t\rightarrow c}$ = 0.49 for *t*-St gives values of 0.46, 0.55, and 0.54 for *p*-BrSt, *m*-BrSt, and *m,m'*-diBrSt, respectively, in adequate agreement with the results in the preceding table. A set of duplicate *m,m'*-diBrSt samples, irradiated for 2 h, gave conversions which were roughly three times those reported for the first experiment in Table VII. Corresponding ϕ_0/ϕ values were in excellent agreement with those in Table VII. It should be noted that, in addition to the usual back-reaction corrections, the conversions in Table VII are corrected for incomplete absorption of the 313-nm incident radiation by the stilbenes in the presence of azulene. In the case of *t-p*-BrSt conversions to *trans*-stilbene were observed which correspond to a minimum quantum yield of 1.2 × 10^{-2} for carbon–bromine bond breaking.

The effect of azulene on 313-nm direct cis → trans isomerization conversions for the stilbenes is shown in Table VIII. Mossy zinc was included in all bromostilbene samples and 1-hexene, 0.40 M, was present only in specified samples. Owing to significant amounts of trans isomer in some of the unirradiated samples, especially in tbe cases of *p*-BrSt and *m,m'*-diBrSt, the more general form

$$\gamma = \gamma_e \ln \frac{\gamma_e - \gamma_0}{\gamma_e - \gamma_t} \quad (1)$$

of the equation suggested by Lamola and Hammond[17] was used in making back-reaction corrections. In eq 1 γ is the net corrected fraction converted and γ_0, γ_t, and γ_e are the initial, final, and photostationary fractions, respectively.

The effect of azulene on 313-nm direct excitation cis → dihydrophenanthrene conversion was determined qualitatively starting with *c-m,m'*-diBrSt. Immediately following sample irradiation optical densities were measured at 463 nm (λ_{max} for diBrDHP) as a function of time directly in the degassed round ampules. First-order decay plots of the net optical densities were extrapolated to zero time to obtain DHP optical densities at the moment the irradiation was stopped. The results are shown in Table IX. First-order rate constants for thermal DHP ring opening did not vary significantly with azulene concentration, $k = (5.6 \pm 1.0) \times 10^{-5}\ s^{-1}$, 24 ± 1 °C. Following dilution optical densities measured at 632 nm showed no change in azulene concentration.

Spectroscopic Observations. Table X lists extinction coefficients for the stilbenes and azulene at 313.0 and 253.7 nm. Absorption spectra of the trans isomers at high concentration were measured in benzene and in methyl iodide. Positions of the first vibrational bands, where discernible, are given in Table XI.

Relative fluorescence intensities measured as a function of temperature in air-saturated *n*-pentane were converted to absolute quantum yields, ϕ_f, using previously published ϕ_f's at 30 °C.[19] Observations from several different experiments were independent of stilbene concentration (within 10%) over the range employed, 6 × 10^{-4} to 2 × 10^{-5} M. Results from representative experiments are shown in Table XII. For *trans*-stilbene optical densities (ODs) were measured at the excitation wavelength in the range 5 to −40 °C in 5 °C intervals. The change in OD was proportional to the change of the density of *n*-pentane:[20] $d/\mathrm{OD} = 4.10_5 \pm 0.02_3$. Correction of ϕ_f's for the change in OD was almost entirely canceled when the refractive index[20] correction ($n_t^2/n_{30°C}^2$) was also applied (values in parentheses in Table XII). Since corrected and uncorrected ϕ_f values fall well within the range of experimental

Table III. Effects of Alkenes and Mossy Zinc on Photostationary States of *m,m'*-Dibromostilbenes with and without Azulene, *n*-Pentane, 313 nm, 30 °C[a]

[St], M × 10^2	[Az], M × 10^2	% $[t]_s$	addend
1.0	0	4.1 ± 0.4[b]	2-methyl-2-butene, 0.01 M
0.11_3	0	4.4 ± 0.5	1-hexene, 0.5 M
0.98	0	4.7 ± 0.2	1-hexene, 0.5 M
1.00	0.78	9.1 ± 0.2	1-hexene, 0.5 M
1.03	1.55	11.7 ± 0.2	1-hexene, 0.5 M
1.04	2.33	13.5 ± 0.3	1-hexene, 0.5 M
1.06	3.11	15.2 ± 0.5	1-hexene, 0.5 M
1.0	0	3.5 ± 0.5[c]	Zn
1.02	0.76	8.5 ± 0.6[d]	Zn
1.06	1.52	11.2 ± 0.6	Zn
1.00	2.28	12.8 ± 0.3	Zn
0.99	3.04	15.0 ± 0.6	Zn
2.50	0	4.9 ± 0.2[e]	Zn
1.00	0.30	5.9 ± 0.1	Zn
1.00	0.60	7.3 ± 0.3	Zn
2.50	1.20	9.3 ± 0.3	Zn
1.00	1.80	10.7 ± 0.4	Zn

[a] Filter systems 2 and 3 unless otherwise indicated. [b] Omission of filter system 3 had no effect on stilbene composition but caused a marked decrease in dibromophenanthrene yield, 3.4 to 0%. [c] As in *b*, 2.6 to 0%. [d] As in *b* for this and following three entries 5.9 to 4.9, 4.7 to 0.7, 3.2 to 0.7, and 3.8 to 0.8%, respectively. [e] Filter system 2; no other products detected by GLC for this and following entries.

Table IV. Azulene Effect on Photostationary States of Direct Stilbene Isomerization, 30 °C, 254 nm, *n*-Pentane[a]

compd	[St], M × 10^2	[Az], M × 10^2	% $[t]_s$
stilbene[b]	1.01	0	51.9 ± 0.5
	1.08	0.105	52.1 ± 0.5
	0.43	1.02_4	56.2 ± 0.6
	0.43	2.04_8	60.1 ± 0.5
p-bromostilbene[c]	1.09	0.106	53.4 ± 0.4[b]
	1.04	0.55_3	61.5 ± 0.3[b]
	1.02	0.75_7	67.8 ± 1.1
	1.02	1.51_4	73.1 ± 0.4
	1.02	2.27	76.0 ± 0.4
	1.02	3.03	78.4 ± 0.2
m-bromostilbene[c]	1.00	0.79	62.1 ± 0.4
	1.01	1.60_6	65.7 ± 0.4
	1.01	2.40_9	68.3 ± 0.4
	1.01	3.21_3	70.3 ± 0.3
m,m'-dibromostilbene	0.63	0.77	70.9 ± 1.2
	1.00	1.51	71.4 ± 0.7
	0.63	1.54	70.7 ± 0.4
	1.00	2.26	72.4 ± 1.0
	0.63	2.31	71.9 ± 1.0
	1.00	3.02	74.1 ± 0.5
	0.63	3.08	73.8 ± 0.5
	1.00	3.77	75.3 ± 0.5
m,m'-dibromostilbene[b,d]	1.03	0	45.9 ± 0.9
	1.02	0.78	61.2 ± 0.5
	1.02	1.57	68.7 ± 0.4
	1.02	2.36	71.8 ± 0.3
	1.03	3.14	74.9 ± 0.6

[a] Filter systems 4 and 5 were employed unless otherwise indicated. [b] Only filter system 4 employed. [c] In one set of solutions it was shown that the Az concentration is not affected by irradiation, GLC, and visible absorption. [d] Over mossy zinc.

Table V. Relative Conversions for the Benzophenone-Sensitized Photoisomerization of the *p*-Bromostilbenes in *n*-Pentane, 366 nm, 30 °C[a]

compd, M × 10^2	% t	% c	$\phi_{c\to t}$	$\phi_{t\to c}$
c-St, 0.0107	2.46 ± 0.09		0.41[b]	
t-p-BrSt, 0.0104		2.97 ± 0.08		0.48
c-p-BrSt, 0.0104	2.80 ± 0.20		0.45	

[a] Benzophenone, 0.05 M throughout; conversions corrected for zero time isomeric contamination and back reaction; filter system 1. [b] Assumed; see text.

uncertainty of the measurements (±5%), no attempt was made to similarly correct ϕ_f values for the other stilbenes. That such correction in *n*-pentane is unnecessary was further demonstrated by measuring the temperature dependence of fluorescence from a degassed *n*-pentane solution of 9,10-diphenylanthracene (ϕ_f = 1.0,[21,22] excitation at 270 nm) in the 30 to −50 °C range. Deviations between normalized fluorescence areas at different temperatures appeared random, the maximum and average deviations being <5 and 1.1%, respectively. Also given in Table XII are approximate fluorescence quantum yields in methylcyclohexane at −195.8 °C. These were ob-

Table VI. Relative Photoisomerization Conversions in *n*-Pentane, 313 nm, 30 °C, Mossy Zn[a]

compd (M × 10^2)	% c[b]	% t[b]	% c[c]	% t[c]	$\phi_{t\to c}$[b]	$\phi_{t\to c}$[c]	$\phi_{c\to t}$[b]	$\phi_{c\to t}$[c]
t-St (1.06)	2.50		2.36		0.49	0.55		
c-St (1.10)		1.72		1.44			0.35	0.35
t-*p*-BrSt (1.04)	2.72		2.36		0.53	0.54		
c-*p*-BrSt (0.99)		3.34		2.04			0.62	0.44
t-*m*-BrSt (1.09)	2.89		2.21		0.59	0.53		
c-*m*-BrSt (1.05)		2.80		1.48			0.55	0.34
t-*m*,*m*′-diBrSt (1.05)	2.85		2.42		0.56	0.56		
c-*m*,*m*′-diBrSt (1.07)		2.03		1.04			0.41	0.24
c-P (2.00)		1.47		1.25			0.55[d]	0.55[d]

[a] Conversions corrected for zero time contamination and back reaction; GLC reproducibility better than ±3%. [b] Filter system 2. [c] Filter systems 2 and 3. [d] Assumed; see text.

tained by measuring relative fluorescence areas for identical solutions at 24.0 °C and at liquid N_2 temperatures. For stilbene the value of $\phi_f = 0.046_5$ measured at 25 °C in methylcyclohexane was used to calculate the tabulated value.[9] For the other stilbenes ϕ_f values at 24 °C were obtained by interpolation from the results in Table XII. Since a solvent change is involved the values for the substituted stilbenes are considered less reliable. As a check of the method employed to obtain these low-temperature ϕ_f's, relative fluorescence quantum yields of 9,10-diphenylanthracene (9,10-DPA) in methylcyclohexane at 24 and −195.8 °C were also measured. The ratio of 0.63 obtained for fluorescence areas at room temperature and in the glass is consistent with the value expected, 0.67, due to elimination of diffusional quenching by oxygen in the glass medium (see below).

Since 253.7- and 313-nm excitation wavelengths were employed in photochemical measurements, approximate fluorescence quantum yields were determined at 24 °C in air-saturated *n*-pentane using these wavelengths. Measurements were carried out in 1-cm^2 cells with OD = 0.0400 for each stilbene at each wavelength. Relative areas of uncorrected fluorescence spectra were converted to ϕ_f values using ϕ_f = 0.040 for *trans*-stilbene (Table XIII).

The effect of oxygen on fluorescence quantum yields of selected compounds is shown in Table XIV.

Discussion

The results reported in this paper can be discussed using the general mechanism in Scheme I, which combines the singlet and triplet paths for stilbene photoisomerization.[7,12] This mechanism has also been applied to the interpretation of related results on nitrostilbenes.[14] In Scheme I $\phi_{1c}{}^{1p}$ is the quantum yield for twisted singlet formation from ^{1}c, $\phi_{is}{}^{1t}$ and $\phi_{is}{}^{1p}$ are intersystem crossing quantum yields from ^{1}t and ^{1}p, k_s and k_t are rate constants for azulene quenching of stilbene singlets and triplets, respectively, and the other symbols have their usual meanings.[25]

Scheme I. Combination of Singlet and Triplet Paths for Stilbene Photoisomerization

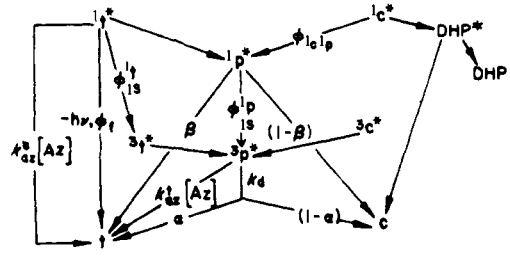

Triplet State Behavior. Benzophenone sensitization affords entry into the stilbene triplet state manifold by diffusion-controlled[7,26] triplet excitation transfer

$$^3B^* + {}^1t \xrightarrow{k_t} {}^1B + {}^3t^* \quad (2)$$

$$^3B^* + {}^1c \xrightarrow{k_c} {}^1B + {}^3c^* \quad (3)$$

where B stands for benzophenone. Transoid and cisoid triplets, ^{3}t* and ^{3}c*, undergo very rapid torsional displacement to a common twisted triplet ^{3}p* as shown in Scheme I. The recent proposal of a barrier between transoid and cisoid geometries whose crossing is slow in comparison to decay to the respective ground states[27] is inconsistent with the temperature independence of benzophenone-sensitized stilbene photoisomerization quantum yields.[4,28] Interaction of relaxed stilbene triplets with quenchers like azulene, having relatively low-lying triplet states, gives trans ground-state molecules as shown in Scheme I. A more detailed mechanism for the functioning of azulene as a triplet excitation acceptor from stilbene is given in the equations:[12,25]

$$^3p^* + {}^1Az \underset{k_{-4}}{\overset{k_4}{\rightleftharpoons}} {}^3[pAz] \quad (4)$$

$$^3[pAz] \underset{k_{-5}}{\overset{k_5}{\rightleftharpoons}} {}^3[tAz] \quad (5)$$

$$^3[tAz] \xrightarrow{k_6} {}^1t + {}^3Az^* \quad (6)$$

Accordingly, k^t_{az} in Scheme I is replaced by the expression

$$k^t_{az} = \frac{k_4K_5(k_6/k_{-4})}{(k_6K_5/k_{-4}) + k_6/k_{-5} + 1} \quad (7)$$

which reduces to

$$k^t_{az} = k_{dif}K_5/(1 + K_5) \quad (8)$$

assuming that k_4, k_{-4}, and k_6 are diffusion controlled and that equilibration step 5 is faster than diffusional separation of the donor-acceptor pair.[25] Since, for benzophenone, $k_c \simeq k_t$ =

Table VII. Azulene Effect on Direct Photoisomerization Conversions of the *trans*-Stilbenes, *n*-Pentane, 313 nm, 30 °C

compd ($M \times 10^2$)	[Az], $M \times 10^2$	% c[a]	f_t[b]	% c[c]	ϕ_0/ϕ
t-St[d]	0	4.69 ± 0.02	1.00	4.82	1.00
(1.03)	0.26_2	3.79 ± 0.07	0.98	3.95	1.22
	0.52_3	3.38 ± 0.04	0.96	3.59	1.34
	1.05	2.59 ± 0.17	0.92	2.86	1.68
	1.57	2.25 ± 0.06	0.88	2.58	1.87
	2.09	1.91 ± 0.14	0.85	2.26	2.13
t-St[d,f]	0	4.64 ± 0.04	1.00	4.77	1.00
(1.00)	0.15	3.87 ± 0.07	0.99	4.00	1.19
	0.30	3.58 ± 0.02	0.98	3.73	1.28
	0.60	3.33 ± 0.08	0.95	3.57	1.34
	1.20	2.58 ± 0.02	0.91	2.88	1.66
	1.80	2.05 ± 0.01	0.87	2.38	2.00
t-St[e,f]	0	1.70 ± 0.02	1.00	1.72	1.00
(1.00)	0.15	1.52 ± 0.03	0.99	1.55	1.11
	0.30	1.49 ± 0.02	0.98	1.53	1.12
	0.60	1.42 ± 0.03	0.95	1.51	1.14
	1.20	1.14 ± 0.03	0.91	1.26	1.36
	1.80	0.99 ± 0.02	0.87	1.14	1.51
t-*p*-BrSt[d,g,h]	0	4.37 ± 0.11	1.00	4.50	1.00
(1.03)	0.22_6	3.65 ± 0.07	0.99	3.78	1.19
	0.56_4	3.31 ± 0.03	0.97	3.49	1.29
	1.13	2.64 ± 0.05	0.94	2.85	1.58
	1.69	2.23 ± 0.02	0.92	2.47	1.82
	2.26	1.66 ± 0.02	0.90	1.87	2.41
t-*m*-BrSt[d,g]	0	5.22 ± 0.06	1.00	5.38	1.00
(1.03)	0.26_5	4.35 ± 0.08	0.98	4.55	1.18
	0.53_0	3.63 ± 0.04	0.96	3.86	1.40
	1.06	3.01 ± 0.07	0.93	3.29	1.64
	1.59	2.25 ± 0.06	0.90	2.54	2.12
	2.12	1.96 ± 0.06	0.87	2.28	2.36
t-*m*,*m*′-diBrSt[d,g]	0	5.14 ± 0.09	1.00	5.28	1.00
(1.03)	0.25_4	3.58 ± 0.07	0.98	3.72	1.42
	0.50_8	2.73 ± 0.08	0.96	2.87	1.84
	1.02	2.00 ± 0.05	0.93	2.17	2.43
	1.52	1.55 ± 0.03	0.90	1.73	3.05
	2.05	1.12 ± 0.04	0.87	1.29	4.09
t-*m*,*m*′-diBrSt[d,f,i]	0	4.80 ± 0.11	1.00	4.91	1.00
(1.00)	0.30	3.03 ± 0.03	0.98	3.13	1.57
	0.60	2.31 ± 0.04	0.96	2.42	2.03
	1.20	1.71 ± 0.01	0.92	1.85	2.65
	1.80	1.25 ± 0.01	0.88	1.41	3.48
t-*m*,*m*′-diBrSt[e,f,i]	0	5.01 ± 0.03	1.00	5.13	1.00
(1.00)	0.15	4.43 ± 0.05	0.99	4.57	1.12
	0.30	3.66 ± 0.01	0.98	3.80	1.35
	0.60	2.78 ± 0.03	0.96	2.93	1.75
	1.20	2.20 ± 0.01	0.92	2.40	2.14
	1.80	1.58 ± 0.03	0.88	1.78	2.88

[a] Net observed conversions. Initial cis isomer content follows: St, 0%; *p*-BrSt, 0.33%; *m*-BrSt, 0.07%; *m*,*m*′-diBrSt, 0%. [b] Fraction of light absorbed by *trans*-stilbenes; see Table X. [c] Conversions corrected for back reaction and incomplete light absorption. [d] Filter system 2 and 3; 40 min irradiation time. [e] Filter system 2. [f] Mossy Zn only. [g] 1-Hexene concentrations in bromostilbene samples 0.54, 0.51, and 0.51 M in the order given. [h] *t*-St formation ~0.12 ± 0.02% in each sample. [i] Initial cis isomer 0.02%.

k_{dif}, the effect of azulene on photostationary state compositions is given by the expression

$$([t]/[c])_s = \alpha/(1-\alpha) + k^t_{az}[Az]/k_d(1-\alpha) \quad (9)$$

Plots of $([t]/[c])_s$ for the bromostilbenes (Table I) against quencher concentration are linear (Figures 1 and 2), as previously reported for stilbene[11,12,25,29,30] and *p*-nitrostilbenes,[13,31] in agreement with eq 9. The values k^t_{az}/k_d and α obtained from the slope and intercept values in Figures 1 and 2 are shown in Table XV. The four- to fivefold drop in k^t_{az}/k_d upon para substitution of a bromine atom has been attributed to an increase in k_d due to heavy-atom enhanced spin-orbit coupling.[7] Such enhancement has been measured directly for transoid triplets. The radiationless decay rate constants measured by flash kinetic spectrophotometry in rigid media

$$^3t^* \rightarrow {}^1t \quad (10)$$

for *t*-St and *t*-*p*-BrSt are 56 and 1.7×10^3 s^{-1} in 3-methylpentane at 77 K and 110 and 2.6×10^3 s^{-1} in glycerol at 195 K, respectively.[32,33] The more modest drop in k^t_{az}/k_d for one and its increase for two *m*-bromo substituents suggest that significant changes in k^t_{az} are also involved.[34] Apparently, the increase in k_d for *m*,*m*′-dibromo triplets is more than compensated for by an increase in K_5 in eq 8. Consequences of this prediction will be the subject of future investigations. Upon changing the solvent from *n*-pentane to benzene, k^t_{az}/k_d values are attenuated by factors of 1.8–2.4, 1.6, 1.4, and 2.3 for St, *p*-BrSt, *m*-BrSt, and *m*,*m*′-diBrSt, respectively. For St and *m*,*m*′-diBrSt these factors are very close to the change in η^{-1}, 2.6, mainly reflecting the effect of viscosity on k_{dif}, eq 8. The smaller factors observed for the other two stilbenes may also reveal some solvent dependence in K_5 and k_d, but are also more uncertain because the smaller k^t_{az}/k_d values in Table XV are more subject to experimental error.

Table VIII. Azulene Effect on Direct Photoisomerization Conversions of the *cis*-Stilbenes, *n*-Pentane, 313 nm, 30 °C

compd (M × 10²)	Az, M × 10²	% t[a]	f_c[b]	% t[c]	ϕ_0/ϕ
c-St[d]	0	1.72 ± 0.02	1.00	1.96	1.00
(2.28)	0.26_7	1.44 ± 0.01	0.93	1.72	1.14
	0.53_3	1.38 ± 0.04	0.87	1.76	1.11
	1.07	1.25 ± 0.02	0.77	1.78	1.10
	1.60	1.20 ± 0.03	0.69	1.89	1.04
	2.13	1.06 ± 0.01	0.62	1.82	1.08
c-St[d,e]	0	3.15 ± 0.10	1.00	3.85	1.00
(2.50)	0.30	3.02 ± 0.08	0.93	3.88	0.99
	0.60	2.86 ± 0.03	0.87	3.84	1.00
	1.20	2.50 ± 0.03	0.76	3.67	1.05
c-St[f]	0	2.07 ± 0.02	1.00	2.27	1.00
(2.50)	0.15	2.07 ± 0.05	0.96	2.35	0.97
	0.30	2.00 ± 0.04	0.93	2.33	0.97
	0.60	1.81 ± 0.02	0.87	2.20	1.03
	1.20	1.70 ± 0.03	0.76	2.32	0.98
	1.80	1.54 ± 0.03	0.68	2.29	0.99
c-*p*-BrSt,[d,g]	0	2.61 ± 0.12	1.00	4.45	1.00
(2.11)	0.26_5	2.70 ± 0.12	0.97	4.41	1.01
	0.52_9	2.83 ± 0.12	0.94	4.55	0.98
	1.06	2.58 ± 0.20	0.89	4.10	1.09
	1.59	2.29 ± 0.20	0.84	3.66	1.22
	2.12	1.93 ± 0.15	0.80	3.13	1.42
c-*m*-BrSt[d,g]	0	4.92 ± 0.10	1.00	7.24	1.00
(2.18)	0.26_5	4.47 ± 0.28	0.94	6.47	1.12
	1.06	4.47 ± 0.15	0.81	7.17	1.01
	1.59	3.96 ± 0.10	0.74	6.67	1.09
	2.12	3.41 ± 0.08	0.68	6.03	1.20
c-*m*,*m*′-diBrSt[d,g]	0		1.00	4.00[h]	1.00[h]
(2.09)	0.26_7	2.01 ± 0.10	0.95	3.56	1.12
	0.53_3	2.05 ± 0.05	0.90	3.36	1.19
	1.07	1.84 ± 0.10	0.82	2.91	1.37
	1.60	1.70 ± 0.11	0.76	2.79	1.43
	2.13	1.55 ± 0.05	0.70	2.67	1.50
c-*m*,*m*′-diBrSt[f]	0	3.17 ± 0.03	1.00	4.97	1.00
(2.50)	0.30	3.04 ± 0.05	0.95	4.44	1.12
	0.60	2.91 ± 0.04	0.90	4.17	1.19
	1.20	2.40 ± 0.02	0.82	3.40	1.46
	1.80	1.91 ± 0.03	0.75	2.79	1.78

[a] Net observed conversions. Initial trans isomer content follows: St, 0.12, 0.11, 0.11%; *p*-BrSt, 2.73%; *m*-BrSt, 0.45%; *m*,*m*′-diBrSt, 1.42 ± 0.05, 0.00%. [b] Fraction of light absorbed by stilbenes; see Table X. [c] Conversions corrected for back reaction and incomplete light absorption. [d] Filter systems 2 and 3; irradiation periods were 2 or 4 h for *c*-St and 4 h for the bromostilbenes. [e] Irradiation period 4.5 h. [f] Filter system 2. [g] 1-Hexene 0.4 M. [h] Sample lost; value obtained by extrapolation of following data.

Similar decay fractions for all the stilbenes are obtained from the intercepts in Figures 1 and 2. There is a consistent small increase in α on changing the solvent from *n*-pentane to benzene. The observed *p*-BrSt isomerization quantum yields with benzophenone as a triplet excitation donor (Table V), $\phi_{c\to t} = 0.45 \pm 0.04$ and $\phi_{t\to c} = 0.48 \pm 0.03$ in *n*-pentane, are in satisfactory agreement with the corresponding value of $\alpha = 0.40$, and their sum is sufficiently close to unity to suggest efficient formation of $^3p^*$ from $^3t^*$ and $^3c^*$. The postulated rapid $^3c^* \rightarrow {}^1c$ conversion[6,10] is accordingly omitted from Scheme I.

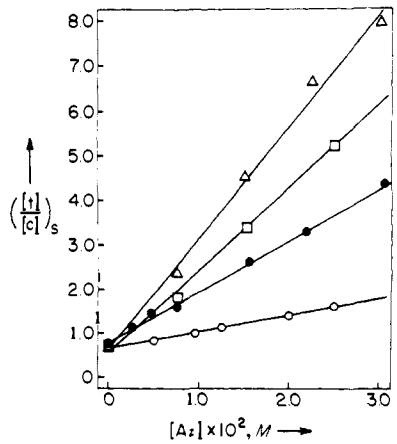

Figure 1. The azulene effect on the benzophenone-sensitized isomerization of St, *p*-BrSt, *m*-BrSt, and *m*,*m*′-diBrSt in *n*-pentane, □, ○, ●, and △, respectively.

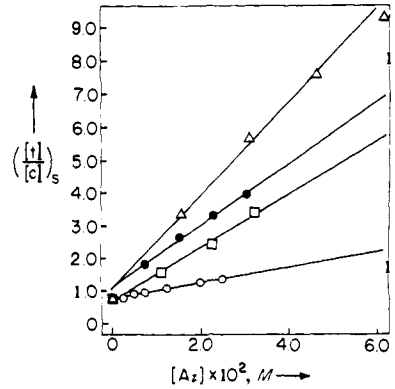

Figure 2. As in Figure 1, but in benzene.

Table IX. Azulene Effect on DHP Formation from *c*-*m*,*m*′-diBrSt[a]

[Az], M × 10^2	OD_0 (463 nm)	f_c[b]	ϕ_0/ϕ
0	0.497	0.91	1.00
0.26_7	0.607	0.86	0.77
0.53_3	0.603	0.82	0.74
1.07	0.631	0.75	0.64
1.60	0.684	0.68	0.55
2.13	0.751	0.63	0.46

[a] Filter systems 2 and 3; solutions and irradiation conditions identical with those in Table VIII. [b] Fraction of light absorbed by *c*-*m*,*m*′-diBrSt based on assumption of 1.5% trans average content.

Singlet State Behavior. Quantum Yields. Average direct photoisomerization quantum yields from Table VI are compared with literature values in Table XVI. For the parent hydrocarbons the agreement between our results and those of Malkin and Fischer[4] is excellent. However, for the bromostilbenes our values are generally larger. In particular we do not find the dramatic decrease in $\phi_{c\rightarrow t}$ for *m*,*m*′-dibromostilbene reported by Krüger and Lippert.[6] Furthermore, Table XVI shows the trans isomers to be significant components in photostationary states obtained with 313-nm irradiation and more so when excitation is at 254 nm where cis and trans isomer extinction coefficients are similar (see Table X). These

Table XIII. Excitation Wavelength Effect on ϕ_f in *n*-Pentane

compd	ϕ_f, 253.7 nm	ϕ_f, 313.0 nm
t-St	0.040[a]	0.040[a]
t-*p*-BrSt	0.036	0.038
t-*m*-BrSt	0.011	0.015
t-*m*,*m*′-diBrSt	0.019	0.020

[a] Intrapolated value from Table XII.

Table X. Extinction Coefficients at Excitation Wavelengths[a]

compd	*n*-pentane		benzene
	$\epsilon_{253.7} \times 10^{-3}$	$\epsilon_{313.0} \times 10^{-3}$	$\epsilon_{313.0} \times 10^{-3}$
t-St	5.28 ± 0.06	19.42 ± 0.32	24.79 ± 0.24
c-St	8.42 ± 0.03	2.51 ± 0.05	3.39 ± 0.02
t-*p*-BrSt	3.93 ± 0.02	31.39 ± 0.42	27.80 ± 0.57
c-*p*-BrSt	8.85 ± 0.05	5.29 ± 0.02	5.45 ± 0.02
t-*m*-BrSt	4.92 ± 0.04	22.43 ± 0.02	23.76 ± 0.14
c-*m*-BrSt	7.81 ± 0.01	2.89 ± 0.04	3.72 ± 0.06
t-*m*,*m*′-diBrSt	4.88 ± 0.04	22.24 ± 0.12	22.99 ± 0.21
c-*m*,*m*′-diBrSt	8.11 ± 0.08	3.49 ± 0.02	4.04 ± 0.02
azulene	15.05 ± 0.30	1.64 ± 0.03	

[a] In M^{-1} cm^{-1}; 24 ± 1 °C.

Table XI. $T_1 \leftarrow S_0$ Absorption of the *trans*-Stilbenes

compd	benzene		methyl iodide	
	$\nu \times 10^{-3}$, cm^{-1}	$\epsilon \times 10^2$, M^{-1} cm^{-1}[a]	$\nu \times 10^{-3}$, cm^{-1}	$\epsilon \times 10^2$, M^{-1} cm^{-1}
t-St[b]	21.4	0.08 (1.02)	16.7	0.08
t-*p*-BrSt	21.0	0.45 (1.50)	19.2	0.45
t-*m*-BrSt	19.6	0.09 (0.95)	18.9	0.65
t-*m*,*m*′-diBrSt	17.0[c]	1.3 (1.5)	17.0[c]	1.5
	21.0[d]	17.6 (29.0)	22.0[d]	31.0

[a] In parentheses are given values of ϵ for that frequency in methyl iodide. [b] Cf. also ref 3. [c] No discernible vibrational structure; absorption onset given. [d] Well-defined shoulder.

Table XII. Temperature Dependence of ϕ_f in *n*-Pentane

t, °C	$\phi_f \times 10^2$ [a]			
	t-St[b]	*t*-*p*-BrSt	*t*-*m*-BrSt	*t*-*m*,*m*′-diBrSt
30.0[c]	3.50 (3.50)	4.37	1.35	1.93
25.0			1.49	
20.0	4.35 (4.31)	4.93	1.64	2.21
11.4			1.93	
10.0	5.41 (5.33)	5.61		2.43
1.4			2.35	
0.0	7.01 (6.86)	6.30		2.69
−9.2			2.88	
−10.0	9.48 (9.22)	7.21		2.94
−20.0	12.4 (12.0)	7.98	3.43	3.26
−30.0	16.7 (15.1)	8.57	4.02	3.60
−40.0	20.9 (20.0)	9.21	4.81	3.93
−50.0	27.9 (26.5)	10.0		4.15
−195.8[d]	95	20	14	5.5

[a] Unless stated otherwise excitation wavelengths are 280, 280, 294, and 296 nm for St, *p*-Br-, *m*-Br-, and *m*,*m*-diBrSt, respectively. [b] Values in parentheses corrected for optical density and index of refraction changes. [c] From ref 19. [d] In methylcyclohexane glass; see text.

Table XIV. Oxygen Effect on ϕ_f

compd	L_0/L[a]	conditions
indeno[2,1-*a*]indene	1.12 ± 0.01	*n*-pentane, air, 27.9 °C
	1.60 ± 0.02	*n*-pentane, O_2, 28.6 °C
t-St	1.00 ± 0.01	*n*-pentane, air, 26 ± 1 °C
	1.02 ± 0.02[b]	*n*-pentane, O_2, 25-28.8 °C
t-*p*-BrSt	1.02 ± 0.03	*n*-pentane, O_2, 28.8 °C
9,10-DPA	1.52 ± 0.02	*n*-pentane, air, 20 °C
	1.50 ± 0.02	methylcyclohexane, air, 20 °C

[a] Ratio of fluorescence intensity in the absence, L_0, and in the presence of oxygen, L. [b] Average of three independent determinations.

Table XV. Triplet State Parameters of the Stilbenes at 30 °C

	n-pentane (0.220 cp)[a]		benzene (0.561 cp)[a]	
compd	α	$k^t_{az}k_d$	α	k^t_{az}/k_d
St[b]	0.36	118 (97)	0.40 (0.41_5)	50 (53)
p-BrSt	0.40	22	0.43	14
m-BrSt	0.45	63	0.53	44
m,m'-diBrSt	0.39	153	0.52	67

[a] N. A. Lange, Ed., "Handbook of Chemistry", 9th ed., Handbook Publishers, Sandusky, Ohio, 1956, pp 1658, 1660. [b] J. Saltiel and B. Thomas, unpublished results and ref 25; values in parentheses from ref 11.

Table XVI. Isomerization Quantum Yields and Photostationary Compositions[a]

compd	$\phi_{t\rightarrow c}$	$\phi_{c\rightarrow t}$[b]	% $[t]_s$	% $[t]_s$[c]
St	0.52 ± 0.03 (0.50)	0.35 ± 0.02 (0.35)	8.3 (7)	52
p-BrSt	0.53 ± 0.03 (0.35)	0.44 ± 0.04 (0.16)	11[d] (−)	55[d]
m-BrSt	0.56 ± 0.04 (0.46)	0.34 ± 0.04 (0.18)	11[d] (6)	59[d]
m,m'-diBrSt	0.56 ± 0.02 (0.53)	0.24 ± 0.04 (<0.05)	4.9[e] (~0)	46[e]

[a] Values in parentheses from ref 4 for St and *p*-BrSt, and from ref 6 for *m*-BrSt and *m,m'*-diBrSt in *n*-hexane. Unless otherwise indicated experiments carried out in *n*-pentane at 30 °C, 313 nm. [b] Values from Table VI without visible light. [c] Excitation at 254 nm. [d] Maximum extrapolated values; see text. [e] Over mossy zinc.

results justify the omission of the proposed[6] $^1c^* \rightarrow {}^3c^* \rightarrow {}^1c$ conversions from Scheme I.

Photostationary States. In preliminary reports[12] bromine's influence on $S_1 \rightarrow T$ spin-orbit coupling was inferred from the photostationary states for direct photoisomerization in the presence of azulene (Tables II and IV). Initial direct excitation experiments with the bromostilbenes were hampered by the formation of bromine atoms which catalyze cis → trans isomerization and consequently give rise to anomalously trans-rich photostationary states, especially in the absence of azulene. Azulene, apparently an excellent bromine atom scavenger, appeared to eliminate this effect. Photostationary states for the bromostilbenes at zero azulene concentration were therefore obtained by extrapolation of linear $([t]/[c])_s$ vs. [Az] plots.[12] A strong positional dependence of radiationless heavy-atom induced spin-orbital coupling was indicated by the analysis of these data.[12] Of the four stilbenes only *p*-BrSt seemed to produce a significant population of triplet states following direct excitation and it was concluded that a bromine atom bonded at the meta position of stilbene is ineffective in inducing $S_1 \rightarrow T$ transitions.[12] Since the temperature dependence of fluorescence quantum yields casts serious doubt on this conclusion (see below), photostationary state measurements for *m,m'*-diBrSt were repeated in the presence of mossy zinc[35] or alkenes[36] as bromine atom scavengers (Tables III and IV and Figure 3). Examination of the data obtained with 313-nm excitation shows that stationary states in the presence of azulene are not seriously affected by the presence of added bromine scavengers. Excitation at 254 nm, on the other hand, gives trans-rich photostationary compositions for [Az] $\lesssim 2.2 \times 10^{-2}$ M, indicating more severe bromine atom interference when the higher energy photons are employed. Zero azulene concentration $([t]/[c])_s$ compositions at 254 nm, obtained earlier by extrapolation,[12] seriously overestimate the presence of the trans isomer.

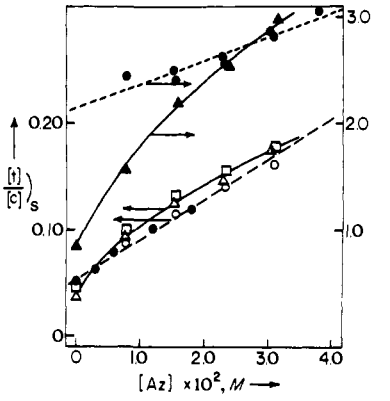

Figure 3. The azulene effect on the direct photoisomerization of *m,m'*-diBrSt in *n*-pentane. Left ordinate is for 313-nm excitation and right ordinate for 254-nm excitation. Dashed lines are for data without added zinc or alkene, closed circles above and open circles below, and correspond to the published preliminary analysis (ref 12). Rectangles are data in the presence of alkenes; triangles and closed circles below are data in the presence of mossy zinc.

The mechanism in Scheme I predicts that photostationary

Table XVII. Calculated Photostationary States at 254 and 313 nm[a]

compd	% $[t]_s$, 254 nm	% $[t]_s$, 313 nm
St	46 (52)	6 (8.3, 7)
p-BrSt	59 (55)	10 (11)
m-BrSt	54 (59)	9 (11.6)
m,m'-diBrSt	49 (46)	9 (4.9)

[a] From eq 13; see text. Values in parentheses are experimental from Table XVI.

[t]/[c] ratios for direct excitation should depend on azulene concentration according to the equation

$$\left(\frac{[t]}{[c]}\right)_s = \left(\frac{\epsilon_c}{\epsilon_t}\right)\phi_{cp}(1 + K_s[Az])$$

$$\times \left\{\frac{\beta(1 - \phi_{is}{}^{1}p)\,(1 + K_t[Az]) + \phi_{is}{}^{1}p\,(\alpha + K_t[Az])}{(1 - \alpha)\phi_{is}{}^{1}t + (1 - \phi_{is}{}^{1}t - \phi_f)\,\{(1 - \alpha)\phi_{is}{}^{1}p + (1 - \beta)\,(1 - \phi_{is}{}^{1}p)\,(1 + K_t[Az])\}}\right\} \quad (11)$$

where $K_s = k^s{}_{az}\tau_{1t}$ and $K_t = k^t{}_{az}/k_d$.[37] In the absence of azulene eq 11 reduces to

$$\left(\frac{[t]}{[c]}\right)_s = \left(\frac{\epsilon_c}{\epsilon_t}\right)\phi_{cp} \times \frac{\beta - (\beta - \alpha)\phi_{is}{}^{1}p}{(1 - \beta)(1 - \phi_f) + (\beta - \alpha)\,\{\phi_{is}{}^{1}p\,(1 - \phi_{is}{}^{1}t - \phi_f) + \phi_{is}{}^{1}t\}} \quad (12)$$

The assumption of identical decay fractions from $^1p^*$ and $^3p^*$, $\alpha = \beta$, reduces eq 12 to

$$\left(\frac{[t]}{[c]}\right)_s = \left(\frac{\epsilon_c}{\epsilon_t}\right)\left(\frac{\phi_{cp}}{1 - \phi_f}\right)\left(\frac{\alpha}{1 - \alpha}\right) \quad (13)$$

The same equation (with α replaced by β) also obtains if the intersystem crossing quantum yields are nearly zero, as is the case for the parent hydrocarbon (see below). In employing eq 13 to predict photostationary states, ϕ_{cp}, the quantum yield of $^1p^*$ formation starting from $^1c^*$ has been taken to be unity.[7,29,38] This assumption neglects competing formation of DHP from $^1c^*$. Provided that $\alpha = \beta$, values for ϕ_{cp} can be estimated from $\phi_{c\rightarrow t}/\alpha$ ratios, although neither the α values in Table XV nor the $\phi_{c\rightarrow t}$ values in Table XVI are considered sufficiently precise. These range from 0.6 for *m,m'*-diBrSt to 1.1 for *p*-BrSt. Another estimate of $\phi_{cp} \leq 0.9$ can be obtained from the reported quantum yield for DHP formation from *c*-St at 0 °C, $\phi_{DHP} \simeq 0.1$.[39] Photostationary compositions calculated using eq 13, $\phi_{cp} = 0.9$, and the data in Tables X, XII, and XV are shown in Table XVII. The largest discrepancy is for *m,m'*-diBrSt at 313 nm, suggesting that in this system the value of $\phi_{cp} = 0.9$ used in the calculation is too large. This is consistent with the observation that upon prolonged irradiation in the presence of mossy zinc formation of phenanthrene appears to occur most efficiently from this stilbene in degassed solutions. The apparent agreement between observed and calculated photostationary compositions suggests that $\alpha \simeq \beta$ for the bromostilbenes as was inferred previously for the parent stilbene.[7,29,38] However, caution is recommended here since initial studies concerning DHP formation give $\phi_{DHP} \simeq 0.22$ for *c*-St at 30 °C.[40] Use of $\phi_{cp} = 0.78$ and the observed $([t]/[c])_s$ at either 254 or 313 nm in eq 13 result in $\beta = 0.46$ for St, which can be compared with $\alpha = 0.36$ from Table XV. Different α and β values have also been obtained for nitrostilbenes.[14,31]

Inspection of eq 11 shows that consecutive quenching of singlet and triplet stilbenes by azulene should result in upwardly concave $([t]/[c])_s$ vs. [Az] plots.[11,12] Since the opposite curvature is experimentally observed in Figure 3, especially for 254-nm excitation, it is clear that eq 11 is at best incomplete. Nonetheless, the sensitivity of $([t]/[c])_s$ ratios to azulene is larger than was previously inferred,[12] reflecting more strongly participation of *m,m'*-diBrSt triplets in the isomerization process. The downward curvature in Figure 3 suggests that at least for the bromostilbenes azulene participates in a competing process which reduces cis → trans quantum yields.

Fluorescence Quantum Yields. The temperature dependence of the fluorescence quantum yields allows estimation of intersystem crossing yields from transoid singlets, $\phi_{is}{}^{1}t$.[7] Such data were available only for *t*-St and *t*-*p*-BrSt in hydrocarbon solvents,[3,5,8] but not in *n*-pentane. Fluorescence quantum yields were therefore determined for all four *trans*-stilbenes in *n*-pentane, the main solvent employed in the photoisomerization studies. 9,10-Diphenylanthracene (9,10-DPA) in *n*-pentane was used as the fluorescence standard. While the fluorescence quantum yield of 9,10-DPA has been reported to be near 1.0 over a wide range of solvents (degassed) and temperatures,[41] its value in *n*-pentane has not been reported. A relatively low value of $\phi_f = 0.89$ at 25 °C has been reported in *n*-heptane, where formation of 9,10-DPA triplets could also be detected.[41] In solvents where $\phi_f < 1.0$, ϕ_f increases and approaches unity as the temperature is decreased.[41-43] Since we find ϕ_f to be temperature independent in degassed *n*-pentane in the range 30 to −50 °C $\phi_f = 1.0$ was assumed. If this assumption is incorrect the quantum yields in Table XII may be high by as much as 10% (cf. also ref 23 and 24). Since the temperature dependence of stilbene fluorescence was determined in the presence of air, measurements were made to determine whether oxygen quenches stilbene fluorescence. The results in Table XIV show that such quenching is not important at room temperature for either *t*-St or *t*-*p*-BrSt. Since oxygen quenching is expected to diminish as the temperature is decreased, owing to its T/η dependence,[42] this effect can be neglected throughout the temperature range in Table XII, despite the accompanying increase in the lifetime of $^1t^*$.

The mechanism in Scheme I predicts that the temperature dependence of stilbene fluorescence should be given by

$$\phi_f = k_f/(k_f + k_{is}{}^{1}t + A_{tp}e^{-E_{tp}/RT}) \quad (14)$$

which can be rearranged to

$$\ln(\phi_f{}^{-1} - \kappa) = \ln(A_{tp}/k_f) - E_{tp}/RT \quad (15)$$

where $\kappa = 1 + k_{is}{}^{1}t/k_f$ and A_{tp} and E_{tp} are Arrhenius parameters for the $^1t^* \rightarrow {}^1p^*$ twisting process. Use of expression 15, first applied to stilbene by Dyck and McClure,[3] has been criticized[44] because it predicts very short stilbene fluorescence lifetimes

$$\tau_f = (k_f + k_{is}{}^{1}t + A_{tp}e^{-E_{tp}/RT})^{-1} \quad (16)$$

at moderate temperatures,[45] which appear to be in conflict with the much larger fluorescence lifetimes (~1.5 ns) reported by Birch and Birks.[44] These authors suggested very rapid equilibration between $^1t^*$ and $^1p^*$ and assumed that essentially all emission occurs after this equilibration is achieved.[44] Quantitative analysis of the temperature dependence of the fluorescence quantum yields, including the $^1p^* \rightarrow {}^1t^*$ process in Scheme I, has shown that the assumption of fast equilibration is not justified and that, if the Birch and Birks lifetimes were correctly assigned to stilbene fluorescence, they would be associated with a minor delayed component.[46] That even this analysis overestimates the contribution of the delayed component has been shown by more recent *t*-St fluorescence lifetime measurements, employing faster instrumentation, which fail to reveal the long-lifetime component even at 60 °C, giving single exponential decay rate constants entirely consistent with

Table XVIII. Parameters for Equation 15

compd	$(A_{tp}/k_f) \times 10^{-4}$	E_{tp}, kcal/mol	κ	ϕ_f^0
t-St[a]	3.1_0 (2.1_8)	4.2_3 (4.0_2)	1.40 (1.05)	0.71 (0.95)
t-*p*-BrSt	0.85	3.8_4	8.6	0.12
t-*m*-BrSt	5.25	4.0_8	13.1	0.07_6
t-*m*,*m*′-diBrSt	0.56_3	3.1_0	18.8	0.05_3

[a] Values in parentheses obtained by setting $\kappa = 1.05$.

Table XIX. Intersystem Crossing Quantum Yields for ^{1}t* at 30 °C

compd	k_f[a,b]	k_{is}^{1t} [a]	A_{tp}[c]	E_{tp}[d]	κ	ϕ_{is}^{1t}	ref
t-St	5.9		1.83	4.23	1.40	0.014	*b*
		<1	1.29	4.02	1.05	0.002	*b*
			0.11	3.06	1.04	0.002	3
			0.74	3.76	1.05	0.002	8
t-*p*-BrSt	6.6	50	0.561	3.84	8.6	0.33	*b*
			0.099	2.69	10	0.33	3
			0.0019_5	0.67	5.7	0.33	4[e]
t-*m*-BrSt	6.0	71	3.15	4.08	13.1	0.17	*b*
t-*m*,*m*′-diBrSt	5.8	104	0.327	3.10	18.8	0.34	*b*

[a] Units: $\times 10^{-8}$ s^{-1}. [b] From ref 19. [c] Units: $\times 10^{-13}$ s^{-1}. [d] Units: kcal/mol. [e] The method of Kirby and Steiner[59] was used to obtain the parameters in eq 14.

eq 15 and 16.[47] Short experimental lifetimes are also consistent with the absence of an oxygen fluorescence quenching effect (Table XIV). It should be noted that in the case of the rigid

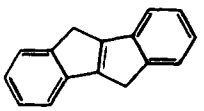

1

trans-stilbene analogue, indeno[2,1-*a*]indene (**1**), whose fluorescence lifetime is $k_f^{-1} \simeq 1.7$ ns,[12,48] oxygen quenching is readily observed.[49]

Two recent laser kinetic investigations of the time dependence of visible-light absorption by electronically excited stilbene transients with lifetimes in the picosecond range complement the fluorescence measurements.[51,52] In the first of these investigations the absorption monitored is assigned to ^{1}p*.[51] An initial fast decrease in transmission is associated with its formation, ^{1}t* → ^{1}p*, a subsequent slow recovery of transmission to its decay. Consistent with this interpretation, the former is temperature dependent, −40 to 20 °C, giving $A_{tp} = 5 \times 10^{11}$ s^{-1} and $E_{tp} = 1.4$ kcal/mol in dimethylformamide, while the latter is temperature independent, $k_d^{1p} = 1.5 \times 10^9$ s^{-1}, in chloroform and dimethylformamide.[53,54] The low values of A_{tp} and E_{tp} are probably due mainly to compensation between these parameters (compare with values in Table XIX). They may also reflect the high stilbene concentration employed, 0.2 M. At this concentration quenching of ^{1}t* by ^{1}t is significant,[55] probably accounting for the fact that the decay rate constants assigned to k_{tp}, $2-3 \times 10^{10}$ s^{-1} at 30 °C in the three solvents studied, are somewhat higher than those obtained from steady-state[46] and transient[47] fluorescence measurements. In the second laser study a short excitation pulse at 3075 Å was utilized and absorption was monitored at 6150 Å.[52] An instantaneous rise in absorption is observed with both stilbene isomers in *n*-hexane, followed by partial relaxation to a lower, constant (in the picosecond time scale) absorption. For *trans*-stilbene the initial absorption, assigned to ^{1}t*, decays with a rate constant of 1.9×10^{10} s^{-1}. The residual absorption has a lifetime on the order of nanoseconds and is assigned to ^{1}p*. The rate constant for ^{1}t* decay is again on the high side (the temperature is not given). The concentration of stilbene, $\sim 3 \times 10^{-3}$ M, inferred from the optical density at 3075 Å, seems too low for self-quenching to be significant in this case. Although these studies have been interpreted as supporting the Birch and Birks model for stilbene photoisomerization,[51,52,56] it is clear that they do not require the key assumption of rapid equilibration between ^{1}t* and ^{1}p* configurations. As indicated above this assumption has not stood the test of more recent fluorescence lifetime measurements.[47]

In applying eq 15 to the fluorescence data k_{is} and k_f are assumed to be temperature independent. A small change in k_f, less than 20% for the 83–333 K range, is likely owing to its probable dependence on the refractive index, *n*, of the medium.[46,57] Variation in the experimental k_f values appears random (average $k_f = 6 \times 10^8$ s^{-1}) and though it does not bear out this expectation is too large to rule it out.[47] While an n^2 dependence for k_f could easily be included in the treatment,[46] its inclusion does not seriously affect the values of the parameters κ, E_{tp}, and A_{tp}/k_f,[46] and is unnecessary for the purposes of this work. Fitting of eq 15 to the ϕ_f values in Table XII in the 30 to −50 °C range was carried out using DeTar's GENLSS iterative least-squares computer program.[58] Best fit parameters are given in Table XVIII. The limiting predicted values of ϕ_f, $\phi_f^0 = \kappa^{-1}$, also given in Table XVIII, may be compared with ϕ_f values at 77 K (Table XII). Except for *m*,*m*′-diBrSt, the observed values are higher, possibly owing to a small temperature dependence in k_{is}^{1t}. Activation parameters obtained with $\kappa = 1.05$ for *t*-St are also given in the table since, in this case, there is ample evidence for a limiting ϕ_f value between 0.9 and unity.[8,46] Use of the corrected *t*-St ϕ_f values (Table XII) and $\kappa = 1.05$ gives $A_{tp}/k_f = 1.80 \times 10^4$ and $E_{tp} = 3.91$ kcal/mol. The fluorescence quantum yields of Sharafi and Muszkat[8] (−100 to 20 °C) in 1:1 methylcyclohexane/methylcyclopentane give $A_{tp}k_f = 0.93 \times 10^4$ and 1.26×10^4 and $E_{tp} = 3.60$ and 3.76 kcal/mol for κ values of 1.05 and 1.11, respectively, in excellent agreement with parameters obtained from the lifetime measurements.[47]

Previously reported limiting ϕ_f^0 values for *t*-*p*-BrSt are 0.12 and 0.17 in methylpentanes[3] and 1:1 methylcyclohexane/isohexane,[4] respectively. While the agreement between activation parameters for *p*-BrSt obtained by different workers is unsatisfactory, compensation in ln $(A_{tp}k_f)$ and E_{tp} and κ values leads to prediction of experimentally indistinguishable intersystem crossing quantum yields at 30 °C. This can be seen in Table XIX, where ϕ_{is}^{1t} values at this temperature are cal-

culated using the equation

$$\phi_{is}{}^{1t} = (\kappa - 1)/[\kappa + (A_{tp}k_f)e^{-E_{tp}/RT}] \quad (17)$$

Table XIX also gives A_{tp} values obtained from A_{tp}/k_f ratios using k_f's calculated with the Birks-Dyson relationship.[19] Since the rate constants for intersystem crossing were assumed to be temperature independent, the $\phi_{is}{}^{1t}$ in Table XIX represent minimum values. Nonetheless, the prediction is clear that substantial fractions of electronically excited transoid singlets intersystem cross. Rate constants, $k_{is}{}^{1t}$, for this process can be estimated from the equation

$$k_{is}{}^{1t} = (\phi_{is}{}^{1t}/\phi_f)k_f \quad (18)$$

(Table XIX). A somewhat larger effectiveness in enhancement of intersystem crossing for meta than for para substitution is indicated, consistent with observed (Table XII) and predicted (Table XVIII) low-temperature fluorescence quantum yields. A second meta bromine substituent further enhances the intersystem crossing rate constant. These conclusions are in direct contradiction with the previously inferred positional dependence of the heavy-atom effect, strongly indicating that bromine's influence on spin-orbital coupling *is not diminished* when it is substituted at a near node of the highest occupied and lowest unoccupied π MOs of stilbene ($c_m = 0.0791$ and $c_p = 0.3138$ in Hückel approximation).[12]

The mechanism of lowest triplet population proposed in Scheme I for the isomerization of the bromostilbenes is not entirely consistent with direct measurements of triplet-triplet absorption spectra, triplet lifetimes, and relative triplet yields obtained for *trans-p*-bromostilbene as a function of temperature (−159 to −196 °C in methylcyclohexane/isohexane, 1:1).[60] Since, owing to medium rigidity, $\phi_{t\rightarrow c}$ approaches zero at low temperatures, the triplet absorption spectrum, which is independent of temperature, has been assigned to $^3t^*$ throughout the temperature range.[60] The decrease in triplet lifetime (down to 333 ns), observed over the same temperature range where $\phi_{t\rightarrow c}$ decreases, is attributed to inhibition of $^3t^* \rightarrow {}^3p^*$ twisting. The surprising observation is that, along with the lifetime decrease, there is a sharp decrease in the signal for $^3t^*$ absorption. It follows that the unactivated radiationless process, labeled $\phi_{is}{}^{1t}$ in Scheme I and Table XIX, which competes with fluorescence cannot be identified with $^3t^*$ formation. A higher triplet pathway for $^3p^*$ formation has been suggested ($^1t^* \rightarrow {}^3t_h^* \rightarrow {}^3p_h^* \rightarrow {}^3p^*$, where the subscript designates higher energy) which bypasses $^3t^*$.[60] At the lower temperatures $^3t_h^* \rightarrow {}^3p_h^*$ twisting is probably also inhibited allowing for $^3t_h^* \rightarrow {}^3t^*$ internal conversion and observation of $^3t^*$ absorption. A corollary to this interpretation is that, owing either to low transition probabilities or short lifetime, no triplet-triplet absorption corresponding to $^3p^*$ is observed. In view of these results the temperature-independent step competing with fluorescence in the bromostilbenes is probably $^1t^* \rightarrow {}^3t_h^*$.[60]

As can be seen in Table XIX, the A_{tp} parameters for the four stilbenes are in the $(0.3\text{-}3) \times 10^{13}\ s^{-1}$ range while the activation energies for the twisting process are in the 3-4 kcal/mol range in *n*-pentane. Owing to strong compensation between these parameters we do not consider the differences to be experimentally significant.[61] A satisfactory fit of the ϕ_f data to eq 15 is also obtained if the same A_{tp} factor, $1.83 \times 10^{13}\ s^{-1}$ (first entry in Table XIX), is chosen for all four stilbenes and the E_{tp} and κ parameters are adjusted using GENLSS.[58] E_{tp} values of 4.6, 3.7, and 4.2 kcal/mol and κ values of 9.3, 11.2, and 22.1 are obtained for *t-p*-BrSt, *t-m*-BrSt, and *t-m,m'*-diBrSt, respectively, leaving the $\phi_{is}{}^{1t}$ values in Table XIX practically unchanged.

Temperature and solvent dependences of ϕ_f have also been determined for *trans-p,p'*-cyanomethoxy- (CMSt) and *trans-p,p'*-nitromethoxystilbene (NMSt).[62] Except for NMSt in dimethylformamide an activated process competing with fluorescence, having widely ranging activation parameters, is found in all cases. An isokinetic plot of these parameters is fairly linear with a slope of ~0.8. In CMSt the activated process is assigned to $^1t^* \rightarrow {}^1p^*$ twisting, but, in a departure from the above mechanistic conclusions, in NMSt it is assigned to $^1t^* \rightarrow {}^3t^*$ intersystem crossing. The reasoning for this reintroduction of the Dyck and McClure[3] and Fischer[4,5] mechanism specifically for NMSt is based on quenching observations and will be considered further below. At this point it is noted that *A* factors are generally larger for NMSt than for CMSt, reaching a high of $3.1 \times 10^{16}\ s^{-1}$ in toluene. It has been argued that such large *A* factors cannot be associated with a unimolecular process in an isolated solute molecule, but reveal solvent-solute interaction during the radiationless transition.[9] Solvent interference with $^1t^* \rightarrow {}^1p^*$ twisting in stilbenes is known to give rise to enhanced *A* factors and activation energies.[9] On the other hand, the assignment of the activated decay process in NMSt to $^1t^* \rightarrow {}^3t^*$ requires that (1) this process be associated with a geometry change which is fast compared to solvent relaxation times and (2) the *A* factors not reflect inefficiency generally associated with changes in multiplicity. Aside from the temperature-dependent process a substantial fraction of NMSt $^1t^*$ molecules at room temperature undergo temperature-independent radiationless decay. This decay too has been assigned to $^1t^* \rightarrow {}^3t^*$ intersystem crossing,[14,16] but in this instance the assignment is entirely consistent with that made above for the bromostilbenes.

Table XX. Intersystem Crossing Quantum Yields for $^1p^*$ at 30 °C

compd	K_s, M^{-1} [a]	$\phi_{is}{}^{1p}$
t-St	29.7	0, 0.34[b]
t-p-BrSt	24.8	1.00[b]
t-m-BrSt	8.3	0.90[b]
t-m,m'-diBrSt	16.4	0.60, 0.82[b]

[a] From ref 19. [b] Without visible light; see text.

Azulene Effect on $\phi_{t\rightarrow c}$. Since azulene can intercept both singlet and triplet stilbene excited states a complex dependence of trans → cis quantum yields on azulene concentration is predicted for the general case in Scheme I:

$$\frac{\phi_{tc}{}^0}{\phi_{tc}} = \frac{(\{[(1-\beta) + (\beta-\alpha)\phi_{is}{}^{1p}](1 - \phi_{is}{}^{1t} - \phi_f) + (1-\alpha)\phi_{is}{}^{1t}\}(1 + K_s[Az])(1 + K_t[Az]))}{\{(1-\alpha)[\phi_{is}{}^{1t} + \phi_{is}{}^{1p}(1 - \phi_{is}{}^{1t} - \phi_f)] + (1-\beta)(1-\phi_{is}{}^{1p})(1 - \phi_{is}{}^{1t} - \phi_f)(1 + K_t[Az])\}} \quad (19)$$

Excepting $\phi_{is}{}^{1p}$ and K_s, experimental values for all the quantities in eq 19 are given in the preceding tables. K_s values derived from a careful study of stilbene fluorescence quenching by azulene were reported previously.[19] Best values of $\phi_{is}{}^{1p}$ were assumed to be those for which the best adherence of the trans → cis quantum yield ratios (Table VII) to eq 19 is obtained (Table XX), assuming that $\alpha = \beta$. Figures 4 and 5 show plots of data for the two extreme cases: *t*-St, $\phi_{is}{}^{1p} = 0\text{-}0.34$, and *t-p*-BrSt, $\phi_{is}{}^{1p} = 1.0$, along with calculated responses to azulene expected for the two limiting cases: no triplet participation, $\phi_{is}{}^{1t} \simeq \phi_{is}{}^{1p} = 0$, eq 20, and complete triplet participation, eq 21.

$$\frac{\phi_{tc}{}^0}{\phi_{tc}} = 1 + K_s[Az] \quad (20)$$

$$\frac{\phi_{tc}{}^0}{\phi_{tc}} = (1 + K_s[Az])(1 + K_t[Az]) \quad (21)$$

It is readily seen that the data for *p*-BrSt are in excellent agreement with the all-triplet mechanism (Figure 5). It has been shown previously[11] and confirmed in this work that experimentally indistinguishable $([t]/[c])_s$ photostationary state

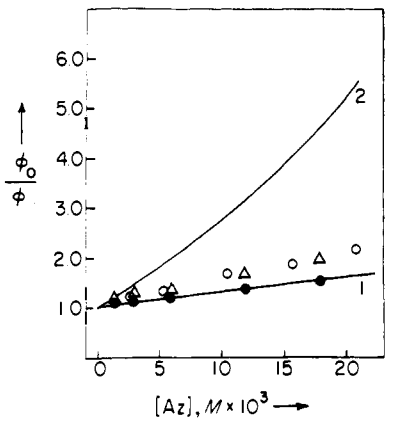

Figure 4. The azulene effect on $\phi_{t\rightarrow c}$ for the direct photoisomerization of *trans*-stilbene. Lines 1 and 2 are calculated using eq 20 and 21, respectively, and the points are experimental; see text.

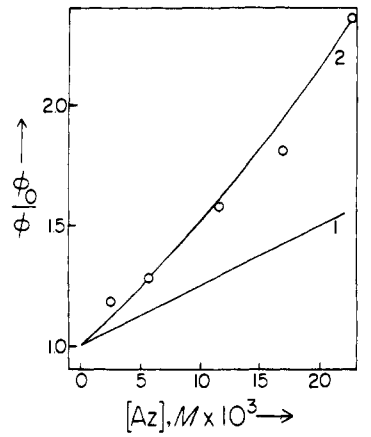

Figure 5. The azulene effect on $\phi_{t\rightarrow c}$ for the direct photoisomerization of *trans*-*p*-bromostilbene. Lines 1 and 2 are calculated using eq 20 and 21, respectively, and the points are experimental.

compositions are obtained when samples are excited at 313 nm, or simultaneously in the visible region, $\lambda \geq 450$ nm. Visible excitation minimizes steady-state concentrations of DHPs. Since DHPs form from the cis isomers, they were not expected to interfere in trans → cis measurement and consequently initial experiments were carried out in the absence of visible excitation. Later measurements were also made in the presence of visible light for *t*-St and *t*-*m*,*m*′-diBrSt. Surprisingly, under these conditions diminished quenching was observed on $\phi_{t\rightarrow c}$ giving rise to the smaller $\phi_{is}{}^{1}p$ values in Table XX. We can offer no satisfactory explanation for this phenomenon, and it is possible that similar experiments with *t*-*p*-BrSt and *t*-*m*-BrSt will also give lower estimates of $\phi_{is}{}^{1}p$. At this point it seems safe to conclude that large fractions of ^{1}t* bromostilbene molecules which do not intersystem cross, owing to the rapid twisting process, do so from ^{1}p*. If, as the above results suggest, the $\phi_{is}{}^{1}p$'s are truly somewhat smaller for the *m*-bromostilbenes than for *p*-bromostilbene, this need not reflect a positional dependence of the heavy-atom effect on intersystem crossing from ^{1}p*. Rate constants for the ^{1}p* → ^{3}p* process in the bromostilbenes cannot be estimated from $\phi_{is}{}^{1}p$'s since the lifetimes of the corresponding electronically excited ^{1}p* states are not known. The fact that ^{1}p* molecules undergo spin-forbidden decay (bromine's effect notwithstanding) does suggest a substantial lifetime for molecules in this conformation. This conclusion is relevant to the notion of regarding the twisted geometry of olefins as holes[63] or funnel points[64,65] in the potential energy surfaces of their lowest excited states.

In contrast to the results for the bromostilbenes, results for *t*-St are close to the no triplet participation limiting case (Figure 4). Values of $\phi_{is}{}^{1}p$ of 0 and 0.34 are estimated for data with and without visible light, respectively. Since laser flash spectroscopy has failed to reveal triplet formation following direct excitation of *t*-St in solution at room temperature,[13] it is likely that $\phi_{is}{}^{1}p$ is close to the lower limit of zero. As indicated above a transient absorption observed in chloroform and dimethylformamide, $k_d = 1.5 \times 10^9$ s^{-1},[51,53] is probably due to ^{1}p*. If $k_d{}^{1}p \simeq 1.5 \times 10^9$ s^{-1} in *n*-pentane also, a maximum $k_{is}{}^{1}p \leq 5 \times 10^8$ s^{-1} can be estimated from the larger $\phi_{is}{}^{1}p$ value for *t*-St in Table XX. For comparison, the rate constant for the related ^{3}p* → ^{1}p crossing in stilbene is only ~1.2×10^7 s^{-1}.[25]

Azulene Effects on $\phi_{c\rightarrow t}$ and $\phi_{c\rightarrow DHP}$. The time dependence of singlet excited state absorption has been measured for *cis*-stilbene in *n*-hexane solution.[52] A very fast initial decay, $\tau = 7 \pm 1$ ps, has been associated with the ^{1}c* → ^{1}p* intramolecular process but must also reflect the competing formation of DHP. The formation of an additional absorbing species of unspecified lifetime and electronic excitation is suggested by the observation of a larger residual absorption in *c*-St than in *t*-St measurements (0.55 and 0.15 of initial value, respectively).[52] This short lifetime of ^{1}c* is consistent with the fact that fluorescence has thus far not been reported from *cis*-stilbene in fluid solutions.[66] It follows that no significant quenching of ^{1}c* by azulene is expected. The mechanism in Scheme I then predicts that intersystem crossing from ^{1}p* should be reflected in an increase of $\phi_{c\rightarrow t}$ with azulene concentration:

$$\phi_{c\rightarrow t} = \phi_{cp}\left\{(1 - \phi_{is}{}^{1}p)\,\beta + \left(\frac{\alpha + K_t[Az]}{1 + K_t[Az]}\right)\phi_{is}{}^{1}p\right\} \quad (22)$$

Examination of the ϕ_0/ϕ values in Table VIII shows that, in the case of *c*-St, $\phi_{c\rightarrow t}$ is independent of azulene concentration as expected for $\phi_{is}{}^{1}p \simeq 0$. In contrast to *t*-St, with *c*-St this result is obtained with or without simultaneous irradiation in the visible region. Using eq 22 it can readily be shown that, for $\phi_{is}{}^{1}p = 0.34$, $(\phi_{c\rightarrow t}{}^{0}/\phi_{c\rightarrow t}) \simeq 0.70$ instead of the observed ratio of 1.0 is predicted for $[Az] \simeq 1.8 \times 10^{-2}$ M. Thus the conclusion that intersystem crossing is not a significant decay process from the ^{1}p* conformation of stilbene appears strengthened. Furthermore, preliminary observations indicate that *c*-St → DHP quantum yields are not affected by azulene in the concentration range employed in the cis → trans experiments.[40]

For the bromostilbenes the large values of $\phi_{is}{}^{1}p$ inferred above lead to the prediction of substantial decreases in $\phi_{c\rightarrow t}{}^{0}/\phi_{c\rightarrow t}$ values with azulene concentration. The opposite trend is generally observed. Here, then, lies, at least in part, the reason why photostationary composition responses to [Az] led to incorrect inferences concerning intersystem crossing efficiencies in the bromostilbenes.[12] The mechanism in Scheme 1 is at best incomplete in describing the photoisomerization of these substituted stilbenes in the cis → trans direction. Since the arguments raised above against substantial quenching of ^{1}c* apply with similar force to the bromostilbenes, there must be at least one additional pathway leading from *cis*- to *trans*-bromostilbenes which, being quenched rather than enhanced by azulene, gives rise to the observed net quenching effects. Two possibilities suggest themselves, both involving electronically excited DHP. In the first, given in Scheme II, formation of DHP in an excited singlet state, ^{1}DHP*, is reversible. This state then serves as a reservoir from which ^{1}c* or ^{1}p* molecules form. Quenching ^{1}DHP* reduces the fraction of molecules which reach ^{1}p*, thus diminishing $\phi_{c\rightarrow t}$. This mechanism does not seem tenable since it should also apply to unsubstituted stilbene, for which Scheme I adequately accounts for the data. The second possibility is given in Scheme

Scheme II. Quenching of ^{1}DHP*

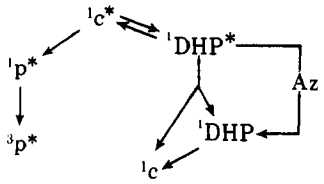

Scheme III. Quenching of ^{3}DHP*

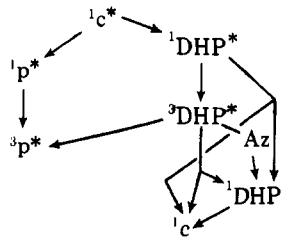

III. Here, bromine substitution enhances intersystem crossing in ^{1}DHP* giving rise to dihydrophenanthrene triplets, ^{3}DHP*, which in the absence of quenchers ring open to give stilbene triplets. Excitation transfer from ^{3}DHP* to azulene diverts molecules which may have reached the *t*-St ground state to ^{1}DHP and eventually ^{1}c. The failure of stilbene triplets to yield ^{1}DHP in sensitized experiments[29] suggests that the key step in Scheme III, ring opening of ^{3}DHP*, is energetically favorable. Qualitative observations with *c-m,m'*-diBrSt reveal strong ^{1}DHP formation enhancement in the presence of azulene (Table IX). Since photostationary ^{1}DHP concentrations were not determined, back-reaction corrections could not be applied to these data which, consequently, may represent a minimum estimate of the enhancement. Quantitative studies of this effect are in progress,[40] but these initial observations support the involvement of electronically excited DHP (probably triplets) as intermediates in the cis → trans photoisomerization. Formation of electronically excited DHP in the cyclization process of ^{1}c* has been postulated before.[67] In addition to providing an explanation for the quenching effects, the behavior of excited DHPs may also account for the significantly higher $\phi_{c\to t}$ values obtained for the bromostilbenes upon simultaneous excitation in the visible region (Table VI). According to Scheme III excitation of ^{1}DHP should increase the yields of the *trans*-bromostilbenes. In the case of stilbene itself, where the ^{1}DHP* → ^{3}DHP* process is probably inefficient, no such $\phi_{c\to t}$ enhancement is expected and none is observed.

The equation

$$\left(\frac{[t]}{[c]}\right)_s = \frac{\epsilon_c}{\epsilon_t}\frac{\phi_{c\to t}}{\phi_{t\to c}} \qquad (23)$$

relates photostationary states to quantum yields. It can be converted to

$$\left(\frac{[t]}{[c]}\right)_s^{Az} \Big/ \left(\frac{[t]}{[c]}\right)_s^{0} = \left(\frac{\phi_{t\to c}^{0}}{\phi_{t\to c}}\right) \Big/ \left(\frac{\phi_{c\to t}^{0}}{\phi_{c\to t}}\right) \qquad (24)$$

which relates photostationary state and quantum yield quenching effects. The agreement between observed and predicted photostationary state compositions in the presence of azulene, while not spectacular, is adequate. An application of eq 24 is shown in Table XXI.

Returning now to the NMSt system, the reasoning for assigning the activated process competing with fluorescence to intersystem crossing rather than twisting can be examined.[14] It is based on the observation of much larger ferrocene quenching in the trans → cis than enhancement in the cis → trans direction for the direct excitation, precluding exclusively common intermediates (^{1}p*, ^{3}p*) for the isomerization in the two directions. As discussed above the bromostilbene results are substantially the same, with the problem in the cis → trans direction being more severe. Quenching to no effect is obtained instead of the expected enhancement which is seen in part for NMSt.[14] Since the nitro group enhances intersystem crossing a combination of Schemes I and III could also obtain for this system. Involvement of DHP in the isomerization of NMSt has been discounted owing to the low quantum yields of DHP formation from the cis isomers of *m*- and *p*-nitrostilbenes, $\phi < 0.001$.[68] However, such low quantum yields could be due to efficient intersystem crossing in the nitro-^{1}DHP*s followed by ring opening in the triplet state (Scheme III). The likely involvement of n,π* states associated with the nitro group in NMST may introduce features in the decay of its excited states which, being absent in the bromostilbenes, make a comparison between these systems less than perfect. More experiments are required before a clear choice between mechanisms can be made.

Table XXI. Observed and Predicted Photostationary State Ratios for *m,m'*-diBrSt, *n*-Pentane

[Az] × 10², M	$([t]/[c])_s^{Az}/([t]/[c])_s^0$ obsd		predicted	
0	1.00[a]	1.00[b]	1.00[c]	1.00[d]
0.30	1.22	1.41	1.21	1.39
0.60	1.53	1.79	1.47	1.68
1.20	1.99	2.27	1.47	1.89
1.80	2.33	2.70	1.62	2.38

[a] Last entries in Table III, 313 nm. [b] Last entries in Table IV interpolated, 254 nm. [c] Values from Tables VII and VIII, filter system 2. [d] As in *c*, filter systems 2 and 3.

Experimental Section

Materials. *trans*-Stilbene, K & K scintillation grade, was recrystallized twice from ethanol and sublimed twice, or, Aldrich, zone-refined, was used without purification. *cis*-Stilbene was either Aldrich research grade, distilled on an 18-in. Nester/Faust spinning-band column, or was obtained by the pyrene-sensitized isomerization of the trans isomer and purified as previously described.[11] In initial experiments with *trans-p*-bromostilbene a sample supplied by Professor F. B. Mallory was employed. *trans*- and *cis-p*-bromostilbenes and the *m*-bromo isomers were synthesized using the Wittig reaction,[69] from the *p*- and *m*-bromobenzyl bromides, Aldrich reagent grade, benzaldehyde, Eastman reagent grade, and triphenylphosphine, Eastman reagent grade. The stilbenes were purified by alumina chromatography followed by recrystallization (twice from cyclohexane or ethanol), sublimation of the trans isomers, and molecular distillation at reduced pressure of the cis isomers. *trans-m,m'*-Dibromostilbene was synthesized by the pyrolysis of the corresponding azine.[70] The azine was prepared from *m*-bromobenzaldehyde, Aldrich, 97%, and hydrazine hydrate, Matheson Coleman and Bell, 99-100%. Cleaner reactions and improved yields (up to 70%) were obtained by employing refluxing diphenyl ether, Aldrich, 99%, distilled under vacuum, as solvent for the pyrolysis of the azine. The stilbene was purified as described above for the monobromo isomers. It was converted to *cis-m,m'*-dibromostilbene by irradiation through Pyrex of a cyclohexane solution (~2 g in 1700 mL) through which was bubbled a constant stream of prepurified nitrogen. A 200-W Hanovia reactor was employed and the progress of the reaction was followed by GLC analysis; up to 90% conversions were obtained. In some cases mossy zinc was included in the bottom of the reaction vessel. The *cis-m,m'*-dibromostilbene was purified by chromatography on alumina, Merck, EM reagent, basic, activity 1. All cis isomers were oils; trans isomers had mp 123.7-124.8, 85.0-87.0, 139.0-140.5, and 100.0-102.0 °C for *t*-St, *t-p*-BrSt, *t-m*BrSt, and *t-m,m'*-diBrSt, respectively. Benzophenone, Fischer reagent grade, was recrystallized from *n*-pentane and sublimed, mp 48.0-49.0 °C. Azulene, Baker or Aldrich reagent grade, was sublimed twice, mp 99.0-100.5 °C. *cis*-Pentadiene, Columbia reagent grade, was bulb-to-bulb distilled immediately prior to use. 9,10-Diphenylanthracene, Aldrich, was purified by alumina chromatography yielding a white solid, mp 245.0-246.5 °C. In-

deno[2,1-*a*]indene was prepared from ethyl phenylacetate using a modification of the available synthesis.[48,71-73] Benzene, Baker reagent grade, was purified using the Metts procedure of exhaustive photochlorination of saturated impurities.[74] Benzene, Baker spectroscopic grade, was used in spectroscopic measurements. *n*-Pentane, Phillips commercial grade, was washed three times with fuming sulfuric acid, Baker reagent grade, three times with saturated aqueous sodium bicarbonate, and three times with distilled water, then distilled crudely, passed through silica gel, and finally fractionally distilled using a 13 mm o.d. × 4 ft vacuum jacketed column filled with Helipac packing, Podbielniac Corp. *n*-Pentane, spectral grade from various commercial sources, was passed through alumina or used without purification for spectroscopic and photochemical studies. Different sources and purification methods of *n*-pentane gave the same results. Solvents used as eluents in column chromatography were distilled. Methyl iodide, Baker reagent grade, was distilled over mossy zinc, Baker reagent grade, immediately before use in spectroscopic measurements.

Analytical Procedures. Determination of trans to cis ratios was accomplished by GLC analysis. Sample preparation and conditions for analyses of St samples were as previously described.[11,32] *p*-BrSt photostationary compositions (for sensitized and 313-nm excitation) were determined using a 2 ft × 1/8 in. column of 5% Apiezon M on Chromosorb W. Photostationary measurements for the *m*-bromostilbenes and all quantum-yield measurements were made using a Varian Aerograph Series 2700 gas chromatograph. Matched pairs of 1 ft × 1/8 in. copper columns containing 1.5% Apiezon N and 5% potassium hydride on Chromosorb P were employed. Programming temperature ranges were 120-200 °C for *p*- and *m*-BrSt and 150-230 °C for *m,m*-diBrSt. St could be similarly analyzed by programming from 100 to 180 °C, but better analyses were obtained on previously described columns.[11,32] The recorders, a Sargent Model SR and a Leeds-Northrup Speedomax W, were both equipped with Disc Integrators.

Absorption Spectra. Ultraviolet and visible absorption spectra were recorded at room temperature using a Cary 14 spectrophotometer. Absorption spectra were measured as a function of temperature using either jacketed 1-cm quartz cells through which a thermostated liquid was circulated or by immersion of the cell in *n*-pentane in a Dewar equipped with quartz windows. Infrared spectra were measured on a Perkin-Elmer Model 137 spectrophotometer and NMR spectra were obtained using a Varian A-60 spectrometer.

Fluorescence Spectra. Fluorescence spectra were recorded on a Hitachi MPF-2A fluorescence spectrometer as previously described.[19] Relative ϕ_f values were obtained as a function of temperature using a jacketed cylindrical quartz (Supracil) cell.[19] The jacket was constructed from 13 mm o.d. tubing and the sample placed in the center of the jacket in 4 mm o.d., 3 mm i.d. tubing. The temperature in the sample compartment was controlled by circulating thermostated methanol through the cell jacket. The temperature of the circulating fluid as it exited the cell was monitored with an iron-constantan thermocouple. Fresh samples were introduced and removed from the cell by syringe periodically to avoid changes due to trans → cis isomerization. A plastic cap fitted to the top of the sample cell prevented solvent evaporation. L_0/L values were determined by degassing solutions directly in the jacketed cells using several freeze-pump-thaw cycles, at a considerable sacrifice in shattered cells. Similar results were obtained using a 1-cm fluorescence cell sealed to a Teflon stopcock. The phosphorescence accessory supplied by the manufacturer with the chopper removed was used for recording fluorescence spectra at 77 K.

Irradiation Procedures. Sample preparation and degassing were as previously described.[11] Pyrex ampules 13 mm o.d. were used in sensitized irradiation, 366 nm, and direct irradiations, 313 nm; quartz (Supracil) ampules, 13 or 3 mm o.d., were used for direct irradiations at 254 nm. Only 0.25 mL of solution was employed in the smaller ampules, 3 mL in the larger. Approximately 0.5 g of mossy zinc, Mallinckrodt, analytical grade, was included in the bottom of the ampules as indicated in the Results section. A merry-go-round apparatus[75] was employed for quantum yield measurements and some photostationary-state measurements. Photostationary states were also determined by irradiating ampules strapped to the outer wall of an appropriately light-filtered Hanovia probe. During the irradiation ampules were immersed in a water bath thermostated at 30 °C. Light filter systems 1-5 were as follows: (1) a combination of Corning CS 7-37 and 0-52 glass color filters transmitting the group of mercury lines at 366 nm; (2) a 500-mL solution of potassium perchromate (0.76 g) and potassium carbonate (15.6 g) transmitting a narrow band of light at 313 nm and visible light at $\lambda > 450$ nm; (3) Corning glass filter CS 7-54 which prevents transmission of the visible light in filter system 3; (4) a quartz Hanovia probe equipped with a Vycor sleeve, containing 2 atm of chlorine gas sealed in the cooling jacket, transmitting light at 254 nm; (5) a uranium glass sleeve, OD ≤ 0.06, 400-440 nm, and a solution prepared by diluting 20 g of copper sulfate and 35 mL of concentrated ammonium hydroxide in 500 mL with water. Filter system 5 transmits the 405- and 436-nm Hg lines. With filter systems 1-3 a 450-W Hanovia medium-pressure mercury lamp, L679A, was employed for photostationary-state measurements and a 200-W Hanovia medium-pressure mercury lamp, S654A, was employed for quantum yield determinations. The 450-W lamp was also employed with filter system 5. A Nester-Faust low-pressure mercury lamp was used with filter system 4.

References and Notes

(1) Supported by National Science Foundation Grants GP-7941, GP-24265, and CHE 76-02439. Presented in part at the 173rd National Meeting of the American Chemical Society, New Orleans, La., March 1977, Abstracts, No. ORGN 133.
(2) National Institutes of Health Predoctoral Research Fellow, 1965-1969.
(3) R. H. Dyck and D. S. McClure, *J. Chem. Phys.*, **36**, 2336 (1962).
(4) S. Malkin and E. Fischer, *J. Phys. Chem.*, **68**, 1153 (1964), and earlier papers in this series.
(5) D. Gegiou, K. A. Muszkat, and E. Fischer, *J. Am. Chem. Soc.*, **90**, 3907 (1968).
(6) K. Krüger and E. Lippert, *Z. Phys. Chem. (Frankfurt am Main)*, **66**, 293 (1969).
(7) For a review see J. Saltiel et al., *Org. Photochem.*, **3**, 1 (1973).
(8) S. Sharafi and K. A. Muszkat, *J. Am. Chem. Soc.*, **93**, 4119 (1971).
(9) J. Saltiel and J. T. D'Agostino, *J. Am. Chem. Soc.*, **94**, 6445 (1972).
(10) E. Lippert, *Z. Phys. Chem. (Frankfurt am Main)*, **42**, 125 (1964).
(11) J. Saltiel and E. D. Megarity, *J. Am. Chem. Soc.*, **91**, 1265 (1969); **94**, 2742 (1972).
(12) For preliminary reports see J. Saltiel, D. W.-L. Chang, and E. D. Megarity, *J. Am. Chem. Soc.*, **96**, 6521 (1974); J. Saltiel, D. W.-L. Chang, E. D. Megarity, A. D. Rousseau, P. T. Shannon, B. Thomas, and A. K. Uriarte, *Pure Appl. Chem.*, **41**, 559 (1975).
(13) D. V. Bent and D. Shulte-Frohlinde, *J. Phys. Chem.*, **78**, 446, 451 (1974).
(14) H. Görner and D. Schulte-Frohlinde, *Ber. Bunsenges. Phys. Chem.*, **81**, 713 (1977).
(15) H. A. Hammond, D. E. DeMeyer, and J. L. R. Williams, *J. Am. Chem. Soc.*, **91**, 5180 (1969).
(16) D. Valentine, Jr., and G. S. Hammond, *J. Am. Chem. Soc.*, **94**, 3449 (1972).
(17) A. A. Lamola and G. S. Hammond, *J. Chem. Phys.*, **43**, 2129 (1965); cf. P. J. Wagner in "Creation and Detection of the Excited State", Vol. I, Part A, A. A. Lamola, Ed., Marcel Dekker, New York, 1971, for derivation of kinetic expressions.
(18) J. Saltiel, D. E. Townsend, and A. Sykes, *J. Am. Chem. Soc.*, **95**, 5968 (1973).
(19) A. Marinari and J. Saltiel, *Mol. Photochem.*, **7**, 225 (1976).
(20) G. Egloff, "Physical Properties of Hydrocarbons", Vol. I, Reinhold, New York, 1939, p 33.
(21) I. B. Berlman, "Handbook of Fluorescence Spectra of Aromatic Molecules", 2nd ed., Academic Press, New York, 1971.
(22) This value may be 3-4% high.[23,24]
(23) C. A. Parker and T. A. Joyce, *Chem. Commun.*, 744 (1967).
(24) J. Olmstead III, *Chem. Phys. Lett.*, **38**, 287 (1976), and references cited therein.
(25) J. Saltiel and B. Thomas, *J. Am. Chem. Soc.*, **96**, 5660 (1974).
(26) W. G. Herkstroeter and G. S. Hammond, *J. Am. Chem. Soc.*, **88**, 4769 (1966).
(27) R. Benson and D. F. Williams, *J. Phys. Chem.*, **81**, 215 (1977).
(28) J. Saltiel and B. Thomas, unpublished results.
(29) G. S. Hammond, J. Saltiel, A. A. Lamola, N. J. Turro, J. S. Bradshaw, D. O. Cowan, R. C. Counsell, V. Vogt, and C. Dalton, *J. Am. Chem. Soc.*, **86**, 3197 (1964).
(30) J. Saltiel, *J. Am. Chem. Soc.*, **89**, 1036 (1967); **90**, 6394 (1968).
(31) H. Görner and D. Schulte-Frohlinde, *J. Photochem.*, **8**, 91 (1978).
(32) J. Saltiel, J. T. D'Agostino, W. G. Herkstroeter, G. Saint-Ruf, and N. P. Buu-Hoi, *J. Am. Chem. Soc.*, **95**, 2543 (1973), and references cited therein.
(33) We thank Dr. W. G. Herkstroeter for his unpublished observations on *trans-p*-bromostilbene.
(34) We were initially inclined to attribute the difference in sensitivity of k^t_{az}/k_d to para and meta substitution to a positionally dependent heavy-atom effect on k_d.[12] However, the results in this paper do not support this view.
(35) P. J. Kropp, T. H. Jones, and G. S. Poindexter, *J. Am. Chem. Soc.*, **95**, 5420 (1973).
(36) J. C. Day, M. J. Lindstrom, and P. S. Skell, *J. Am. Chem. Soc.*, **96**, 5616 (1974).
(37) Previous versions[7,12] of eq 11 are in error.
(38) G. S. Hammond and J. Saltiel, *J. Am. Chem. Soc.*, **84**, 4983 (1962).
(39) K. A. Muszkat and E. Fischer, *J. Chem. Soc. B*, 662 (1967).
(40) J. C. Mitchener and J. Saltiel, unpublished results.
(41) G. Heinrich, S. Schoof, and H. Gusten, *J. Photochem.*, **3**, 315 (1974-1975).
(42) W. W. Mantulin and J. R. Huber, *Photochem. Photobiol.*, **17**, 139 (1973).

(43) J. R. Huber, M. A. Mahaney, and W. W. Mantulin, *J. Photochem.*, **2**, 67 (1973-1974).
(44) D. J. S. Birch and J. B. Birks, *Chem. Phys. Lett.*, **38**, 432 (1976).
(45) J. Saltiel, J. T. D'Agostino, O. L. Chapman, and R. D. Lura, *J. Am. Chem. Soc.*, **93**, 2804 (1971).
(46) J. L. Charlton and J. Saltiel, *J. Phys. Chem.*, **81**, 1940 (1977).
(47) M. Sumitani, N. Nakashima, K. Yoshihara, and S. Nagakura, *Chem. Phys. Lett.*, **51**, 183 (1977); we thank Professor Yoshihara for a preprint of this paper; F. Heisel, J. A. Miehe, and B. Sipp, *Chem. Phys. Lett.*, **61**, 115 (1979).
(48) J. Saltiel, O. C. Zafiriou, E. D. Megarity, and A. A. Lamola, *J. Am. Chem. Soc.*, **90**, 4759 (1968).
(49) The possibility that $^1p^*$ is not quenched by oxygen does not seem viable. Interaction of $^1p^*$ with triplet oxygen should give the triplet complex, $^3(pO_2)^*$, which is the intermediate proposed to lead to efficient quenching of $^3p^*$ by oxygen.[50]
(50) J. Saltiel and B. Thomas, *Chem. Phys. Lett.*, **37**, 147 (1976).
(51) E. Heumann, W. Triebel, R. Uhlmann, and B. Wilhelmi, *Chem. Phys. Lett.*, **45**, 425 (1977).
(52) O. Teschke, E. P. Ippen, and G. R. Holton, *Chem. Phys. Lett.*, **52**, 233 (1977).
(53) An anomalously slow $k_d^{1p} = 3 \times 10^7\ s^{-1}$ is reported[51] in ether, suggesting possibly the formation of $^3p^*$ in this solvent.
(54) No information is given in ref 51 concerning degassing of solutions. Oxygen, if present, would be expected to quench $^2p^*$, thus leading to a higher measured value for k_d^{1p*}.[49,50]
(55) Cf., for example, H. Stegemeyer, *Z. Naturforsch. A*, **16**, 643 (1961); *Chimia*, **19**, 535 (1965).
(56) J. B. Birks, *Chem. Phys. Lett.*, **54**, 430 (1978).
(57) Cf., for example, J. Olmstead III, *Chem. Phys. Lett.*, **38**, 287 (1976).
(58) D. F. DeTar, *Comput. Programs Chem.*, **4**, 71 (1972).
(59) E. P. Kirby and R. F. Steiner, *J. Phys. Chem.*, **74**, 4480 (1970).
(60) H. Görner and D. Schulte-Frohlinde, submitted for publication. We are indebted to Professor Schulte-Frohlinde for a preprint of this paper.
(61) J. E. Leffler, *J. Org. Chem.*, **31**, 533 (1966).
(62) M. N. Pisanias and D. Schulte-Frohlinde, *Ber. Bunsenges. Phys. Chem.*, **79**, 662 (1975).
(63) R. C. Dougherty, *J. Am. Chem. Soc.*, **93**, 7187 (1971).
(64) J. Michl in "Chemical Reactivity and Reaction Paths", G. Klopman, Ed., Wiley, New York, 1974, p 301.
(65) H. E. Zimmerman, D. S. Kamm, and D. P. Werthemann, *J. Am. Chem. Soc.*, **96**, 7821 (1974).
(66) G. Fischer, G. Seger, K. A. Muszkat, and E. Fischer, *J. Chem. Soc., Perkin Trans. 2*, 1569 (1975).
(67) Cf., for example, F. B. Mallory and C. W. Mallory, *J. Am. Chem. Soc.*, **94**, 6041 (1972).
(68) H. Jungmann, H. Güsten, and D. Schulte-Frohlinde, *Chem. Ber.*, **101**, 2690 (1968).
(69) L. F. Fieser and M. Fieser, "Reagents for Organic Synthesis", Wiley, New York, 1967, pp 1065 and 1238.
(70) N. P. Buu-Hoi and G. Saint-Ruf, *Bull. Soc. Chim. Fr.*, 955 (1967); 661 (1968).
(71) K. Brand and K. O. Miller, *Ber.*, **55**, 601 (1922).
(72) S. Wawzonek, *J. Am. Chem. Soc.*, **62**, 745 (1940).
(73) C. T. Blood and R. P. Linstead, *J. Chem. Soc.*, 2263 (1952).
(74) L. L. Metts and J. Saltiel, unpublished results.
(75) F. G. Moses, R. S. H. Liu, and B. M. Monroe, *Mol. Photochem.*, **1**, 245 (1969).

Reaction of Vinyl Chloride with Difluorosilylene by Cocondensation

Chao-shiuan Liu* and Tsai-lih Hwang

Contribution from the Department of Chemistry, National Tsing Hua University, Hsinchu, Taiwan, Republic of China. *Received August 3, 1978*

Abstract: The reaction between difluorosilylene and vinyl chloride by cocondensation at −196 °C is studied. Formation of the products is viewed as the result of either ring closure or H migration of a diradical intermediate. The ring-closure process results in two isomers of 4,5-dichloro-1,1,2,2-tetrafluoro-1,2-disilacyclohexane, which are characterized by an analysis of their fluxional behaviors in the ^{19}F NMR spectra. The activation parameter of the cis isomer is obtained and compared with related systems. Relevance of the results of this reaction to an integrated reaction mechanism of insertion vs. addition of oligomeric difluorosilylenes is discussed.

Unlike the well-studied addition reactions with alkynes,[1-3] the study of the addition reaction of difluorosilylene with alkenes has been very limited. Ever since Margrave et al.[4] published their communication on the reaction of difluorosilylene with ethylene, there has been no further work concerning this aspect in the literature in some 12 years. A part of the reason is due to the difficulty in isolating the stereoisomers of the presumably silacyclic products and to the broadened NMR spectra of the products (both ^1H and ^{19}F NMR) which hamper a definite structural characterization of such compounds.[4,5]

We now report the result of the reaction of difluorosilylenes with vinyl chloride which includes, in our view, the well-characterized 1,2-disilacyclohexane derivatives that leave no doubt about the type of structure that Margrave proposed in his first communication.[4]

Experimental Section

A greaseless vacuum system was used for the reaction and for the manipulation of volatile compounds. SiF_2 was prepared and reacted with vinyl chloride in the same manner as has been described previously.[6] All gas reagents were products of Matheson Gas Co. used without further purification.

After the reaction, excess SiF_4 and unreacted vinyl chloride were removed completely from the reaction product mixture by pumping through a trap kept at −64 °C. (In fact, all reaction products are not volatile at −45 °C so there was no loss of any reaction product by this procedure.) After careful fractionation and fractional sublimation under vacuum, three major products were obtained (designated as I, II, and III). Compound III, a colorless crystal of mp 93-94 °C,[7] could be isolated easily because it was not volatile at room temperature. The mixture of compound I and compound II was gently heated (about 40 °C) from the bottom of a vertical column in which compound II, a colorless, crystalline material of mp 37-38 °C, was fractionally sublimed upward while compound I, a colorless liquid, dripped down. The crystalline product collected at the top of the column was II in pure form. However, the liquid left over was found to be a mixture of I and II and remained as it was after all our purification attempts failed. The total yield of the reaction products based on the quantity of vinyl chloride used was estimated to be 25%, exeptionally high for SiF_2 reactions.[2] The relative yields of these three compounds are approximately 10% for I, 50% for II, and 40% for III. The results of elemental analysis are listed in Table I.

^1H, ^{19}F, and ^{13}C NMR spectra were recorded on a JEOL JNM-60HL and a JEOL FX-100 spectrometer operating at 60/56.4 and 25.1 MHz, respectively. IR and mass spectra were obtained from a Perkin-Elmer 580 IR and a JEOL JMS-100 mass spectrometer. The spectral data are summarized in Tables I and II.

Results and Discussion

The mass spectra of the three compounds show the same molecular formula, $C_4H_6Cl_2Si_2F_4$. Chlorine isotope patterns

0002-7863/79/1501-2996$01.00/0